Version of Record: https://www.sciencedirect.com/science/article/pii/S0045653521027259
Manuscript_a6bc8853451b46076c6b5a3f931dc3bf

Prenatal exposure to paraquat and nanoscaled TiO_2 aerosols alters the gene expression of the developing brain

Quentin Hamdaoui[1,2], Yanis Zekri[1], Sabine Richard[1], Denise Aubert[1], Romain Guyot[1], Suzy Markossian[1], Karine Gauthier[1], François Gaie-Levrel[2], Anna Bencsik[3], Frédéric Flamant[1,4]

[1]*IGFL, Functional genomics of thyroid hormone signaling group, Lyon, France*

[2]*Laboratoire national de métrologie et d'essais (LNE), Paris, France*

[3]*Université Claude Bernard Lyon 1, ANSES, laboratoire de Lyon, France*

Corresponding author : Institut de Génomique Fonctionnelle de Lyon, Université de Lyon, CNRS UMR 5242, INRAE USC 1370 École Normale Supérieure de Lyon, Université Claude Bernard Lyon 1, 46 allee d'Italie F-69364 Lyon, France. 00 (33) 4 26 73 13 32 E-mail: Frederic.flamant@ens-lyon.fr

Abstract

Nanopesticides are innovative pesticides involving engineered nanomaterials in their formulation to increase the efficiency of plant protection products, while mitigating their environmental impact. Despite the predicted growth of the nanopesticide use, no data is available on their inhalation toxicity and the potential cocktail effects between their components. In particular, the neurodevelopmental toxicity caused by prenatal exposures might have long lasting consequences. In the present study, we repeatedly exposed gestating mice in a whole-body exposure chamber to three aerosols, involving the paraquat herbicide, nanoscaled titanium dioxide particles ($nTiO_2$), or a mixture of both. Particle number concentrations and total mass concentrations were followed to enable a metrological follow-up of the exposure sessions. Based on the aerosols characteristics, the alveolar deposited dose

© 2021 published by Elsevier. This manuscript is made available under the CC BY NC user license
https://creativecommons.org/licenses/by-nc/4.0/

in mice was then estimated. RNA-seq was used to highlight dysregulations in the striatum of pups in response to the *in utero* exposure. Modifications in gene expression were identified at post-natal day 14, which might reflect neurodevelopmental alterations in this key brain area. The data suggest an alteration in the mitochondrial function following paraquat exposure, which is reminiscent of the pathological process leading to Parkinson disease. Markers of different cell lineages were dysregulated, showing effects, which were not limited to dopaminergic neurons. Exposure to the $nTiO_2$ aerosol modulated the regulation of cytokines and neurotransmitters pathways, perhaps reflecting a minor neuroinflammation. No synergy was found between paraquat and $nTiO_2$. Instead, the neurodevelopmental effects were surprisingly lower than the one measured for each substance separately.

Introduction

In response to the growing worldwide demand for food, nanotechnology applications in agriculture elicit a particular interest, taking the form of innovative nanofertilizers and nanopesticides (NPe). This term mostly refers to either pesticides with nano-sized active substances or mixtures in which engineered nanomaterials (ENM) are mixed with conventional active ingredients to control their transport, release, or degradation (Sun et al., 2019). ENMs are defined as intentionally produced products with any external dimension or an internal surface structure at the nanoscale, i.e., in the 1 - 100 nm size range (ISO/TS 80004-1:2015). Overall, nanopesticides may represent important technological innovations to address the sanitary and environmental drawbacks of pesticides, as they could decrease the required tonnages of active substances. More than 1000 patents linked with these technologies have already been granted in the past years (Kah et al., 2019) and a rapid increase of NPe use is expected (Gilbertson et al., 2020).

Several authors already emphasized the knowledge gap surrounding the sanitary impact of these emerging products (Kah et al., 2018; Sun et al., 2019; Agathokleous et al., 2020) and health agencies highlighted the necessity to assess the toxicological consequences of a deliberate release of ENM in the environment (USDA, 2015). ENMs can cross the placenta (Bongaerts et al., 2020; Guillard et al., 2020) and the brain-blood barrier (Bencsik et al., 2018; Cena and Jativa, 2018; Boyes and van Thriel, 2020) and might thus alter fetal brain development. Subcutaneous administration of $nTiO_2$ into gestating mice notably increases dopamine levels in the cortex and striatum of the offspring (Takahashi et al., 2010; Umezawa et al., 2012). Prenatal exposure to $nTiO_2$ also has long term consequences in rats, enhancing depressive-like behaviors at adult stage (Cui et al., 2014).

ENMs contained in nanopesticides might also exert an adverse effect by potentiating the toxicity of pesticides. Although the current regulation enforces to assess the toxicity of both

ENMs and pesticides, the novel properties arising from their combination is not carefully addressed in current test guidelines (Kookana et al., 2014). However, ENMs can modify the absorption, biodistribution and reactivity of associated chemicals (Naasz et al., 2018). Synergistic hepatotoxicity of a mixture of paraquat (PQ) and SiO_2 nanoparticles has also been reported in mice (Nishimori et al., 2009).

We address here the possible occurrence of synergistic effects induced by the prenatal exposure to aerosols involving a mixture of an active substance and an ENM. As a proof of principle, we associated PQ with TiO_2 P25 ($nTiO_2$), which is both an ENM suitable for agricultural applications (Wang et al., 2016) and a reference toxicological nanomaterial extensively studied in the literature (Shi et al., 2013; Zhang et al., 2015). We prioritized the developmental period because of its high sensitivity to environmental factors (Barouki et al., 2012) and the neurodevelopment because any adverse effect at this stage could have irreversible consequences.

PQ was selected for its known neurotoxicity. Exposures of gestating mice (20 mg/kg/day) provokes irreversible neurobehavioral and cognitive deficits in the offspring (Ait-Bali et al., 2016). Human occupational exposure to PQ is also suspected to increase the occurrence of Parkinson Disease (Kamel et al., 2007; Tanner et al., 2011; Wang et al., 2011; Moisan et al., 2015; Brouwer et al., 2017) . Although the association of PQ and P25 $nTiO_2$ has not been reported in the fields, it might be suitable for agriculture, as the $nTiO_2$ photocatalytic activity can degrade PQ under UV illumination (Florencio et al., 2004; Nicosia et al., 2021). Their association could reduce the half-life of PQ in soils, which otherwise can reach several years (Sartori and Vidrio, 2018).

We chose to expose mice by inhalation, as it is a major route of occupational exposure to pesticides. Depending on the spraying conditions and the volatility of the pesticide formulation, 10-75% of the applied tonnages are unintentionally disseminated in the air

(Pimentel, 2014). As a result, low concentrations of pesticide residues can be detected in air samples of both rural and urban sites (Schummer et al., 2010; Coscollo et al., 2013). In this study, we used an ad hoc aerosol exposure chamber for rodents, which was previously characterized using a metrological protocol, to generate PQ, $nTiO_2$ and PQ + $nTiO_2$ aerosols (Hamdaoui et al., 2021).

Material and methods

Animals and experimental design

Experimentations were conducted according to the European regulation concerning the protection of animals dedicated to scientific purposes (European Directive 2010/63/EU). The protocol was approved by the local Ethics Committee (CECCAPP) and the French Ministry for Research and Higher Education (CECCAPP_ENS_2019_015). Two-month old primiparous C57Bl6/J mice (gestation day 4, GD4, purchased from Charles Rivers) were randomly assigned to hosting cages (2 females/cage) and housed in standard environmental conditions (humidity of 55 ± 10%; temperature 22 ± 2°C; 12/12 h light/dark cycle) at the Plateau de Biologie Expérimentale de la Souris (SFR BioSciences Gerland - Lyon Sud, France Accreditation N° D54-547-10). Animals had free access to water and a supplemented diet for pregnant mice (Safe 105 rodent pellets).

Groups of gestating mice were exposed to aerosols of either PQ (0.1 mg/m³), $nTiO_2$ (10 mg/m³) or PQ + $nTiO_2$ (10 mg/m³). These target concentrations were chosen to match the values of occupational exposures reported in the literature, in $nTiO_2$ production sites (5 mg/m³; particle size in the range of 15 – 710.5 nm) (Lee et al., 2011) and in PQ treated fields (0.12 mg/m³) (Morshed et al., 2010). One additional control group was kept in the same conditions during the duration of the exposure sessions, but without aerosol exposure. Each group of exposure was composed of 12 gestating mice exposed at the same time. Gestating mice were repeatedly exposed from GD6 to GD18 for 1.5 hour, 6 days/ week, for a total of 11

sessions of exposure, including an individual body weight follow-up. Male and female pups received a lethal intraperitoneal injection (6 mL/kg) at post-natal day 14 (PND14) of a mixture of Ketamine (33 mg/mL) and Xylazine (6.7 mg/mL). Blood was collected on ice in heparin tubes, then centrifuged (15 min at 2,500 g) and the supernatants were stored at −80°C. Organs were weighted and sampled, then stored at −80 °C for later analysis. The striatum was dissected and snap frozen in liquid nitrogen.

Aerosol exposures

The aerosols and the exposure chamber used in this study have been previously characterized (Hamdaoui et al., 2021). Briefly, the aerosol exposure chamber was composed of a rodent cage (Tecniplast GR900, internal volume of 19.8 L), used as a whole-body exposure system, coupled with a nebulizer (model 3076, TSI Inc.) to produce aerosols from colloidal suspensions. It was operated to generate three different aerosols i.e., $nTiO_2$ alone, PQ alone and $nTiO_2$ mixed with PQ (PQ + $nTiO_2$). Aerosols were produced from daily prepared colloidal suspensions with PQ dichloride hydrate (Sigma Aldrich reference 856177) in ultrapure water (MilliQ, Millipore, 18.2 MΩ.cm resistivity) and/or bulk powders of $nTiO_2$ (Sigma Aldrich reference718467). All colloidal suspensions were constantly stirred during the nebulization process. The generated $nTiO_2$ aerosols were composed of nanostructured agglomerates and aggregates of $nTiO_2$ nano-objects. The stability of PQ concentration in suspension with $nTiO_2$ was verified, to ensure that our experimental conditions did not cause its photocatalytic degradation during aerosol generations. The metrological characterization of this experimental set-up was previously described in terms of particle number size distribution, mass and number concentrations, spatial and temporal stability (Hamdaoui et al., 2021). The proper functioning of the device and the stability of aerosols were monitored during each animal exposures in real-time, by using a condensation particle counter (model 3007, TSI Inc.) to measure the particle number concentrations inside the exposure chamber.

In addition, the mass concentrations of aerosols were also monitored by aerosol filtration using a 47 mm filter-holder (Pallflex® filters, EmfabTMTX40HI20-205 WW type) followed by gravimetric measurements. The chamber average concentrations did not deviate from the mean by more than ± 20%, in accordance to the test guidelines for inhalation toxicology (OECD, TG 412).

Gestating mice deposited particle mass estimation

The deposition fractions of aerosols in gestating mice and human lungs were calculated using the Multiple Path Particle Dosimetry Model (MPPD version 3.04). Several estimations were necessary to determine the relation between mice model and human exposure by using the alveolar surface as weighting factor (Jarabek et al., 2005). The characteristics of aerosol previously described (Hamdaoui et al., 2021) were used to estimate the alveolar deposition fraction for each aerosol. According to the recommended exposure limit of the National Institute for Occupational Safety and Health (NIOSH) for ultrafine TiO_2 and PQ, 300 µg/m³ was used for $nTiO_2$ and 100 µg/m³ for PQ for the calculation in human. The target concentrations used in this study (10 mg for $nTiO_2$ and 100 µg/m³ for PQ) were chosen for mice, with a minute ventilation of 22.2 mL/min (Tankersley et al., 1994)and an alveolar surface of 0.05 m² (Stone et al., 1992). A scenario of occupational exposure was chosen, involving a woman working for 8 months during pregnancy, with a nasal minute ventilation of 19 L/min, corresponding to workers achieving light duties (Cassee and de Winter-Sorkina, 2003)and a human alveolar surface of 102 m² (Stone et al., 1992). We assumed that this worker would be exposed 8 h per day, 5 days per week, 20 days per month using the Yeh/Schum symmetric lung model without clearance.

Plasmatic markers of inflammation

Systemic inflammation is known to play an important role in neurologic and neurodevelopmental impairments and inflammation is typically measured by quantifying

circulating cytokines. Pups plasma were thawed and pooled by litters (n≥5/litter). Fifty microliters were assayed using an ELISA multiplexed kit (MCYTOMAG-70K-26, Bio-Techne) to measure the concentrations of 8 cytokines (MCP-1, Cxcl1, IL-1 beta, IL-4, IL-6, IL-17, TNF-alpha) and the matrix metalloproteinase MMP12 on a Luminex platform (Luminex MAGPIX, ThermoFisher). These markers were selected for their implication in neurodevelopment (MCP-1, IL-1 beta, IL-6 and TNF-alpha) (Nist and Pickler, 2019), their role as pro-inflammatory factors (IL-4, IL-10, IL-17 and Cxcl1), or in extracellular matrix remodeling (MMP12) following tissues insults. The gene *Mmp12* has already been described as an early marker of the lung insults in response to low concentrations of PQ in mice (Tomita et al., 2007).

RT-qPCR

Total RNA was extracted using RNeasy Mini kit (Qiagen) from frozen striatum (n≥8/group). On column DNase digestion was used to remove contaminating DNA. RNA concentrations were measured with a Nanodrop spectrophotometer (ThermoScientific) and 1 µg of each RNA sample was reverse transcribed in murine leukemia virus reverse transcriptase (Promega) and random DNA hexamer primers. Quantitative PCR was performed according to a standard protocol, using the Biorad iQ SYBRGreen kit and the Biorad CFX96 thermocycler. For each pair of primers (Table S1) a standard curve was established to verify PCR efficiency (90%–110%) and quantification was performed using the $2^{-\Delta\Delta Ct}$ method (Livak and Schmittgen, 2001). We verified that the *Gapdh* and *Rplp0* housekeeping genes which were used as internal controls do not vary significantly in our samples according to RNA-seq (Figure S1). Differences among experimental groups were analyzed with the Kruskal-Wallis test followed by Dunn's post hoc test to compare mRNA relative mean levels using Prism (GraphPad 8.3 Software, Inc, San Diego CA).

RNA-seq analysis

Striatum RNA was extracted using the Macherey-Nagel NucleoSpin RNA II kit. cDNA libraries were prepared using the total RNA SENSE kit (Lexogen, Vienna Austria) and analyzed on an Nextseq500 sequencer (Illumina). Raw data of single-end sequencing (GSE169579) were converted to count tables using htseq-count (Galaxy Version 0.6.1galaxy3) (Anders et al., 2015). Differential gene expression analysis was performed between exposure and control groups with Deseq2 (Galaxy Version 2.1.8.3, one-factor, parametric fit type, automatic outlier replacement and filtering, p-adjusted values <0.05; minimum read number >10) (Love et al., 2015). RNASeq data are accessible through GEO Series accession number: GSE143933 (www.ncbi.nlm.nih.gov/geo/query/acc.cgi?acc=GSE169579#).

Gene Set Enrichment Analysis (GSEA)

Gene Set Enrichment Analysis (https://www.gsea-msigdb.org/gsea/index.jsp) was performed as previously described (Mooney and Wilmot, 2015)Statistical significance was tested by empirical permutation followed by multiple hypotheses correction using Kolmogorov-Smirnov statistics (Subramanian et al., 2005; Tamayo et al., 2016). Several gene set databases were used: hallmark, C2 curated (KEGG, REACTOME) and C5 ontology (biological process) (https://www.gsea-msigdb.org/gsea/msigdb). A p-value cut-off of p <0.01 and an FDR <0.05 were used to select the significant gene sets, and only a limited number was selected to avoid pathway redundancy. Gene sets were filtered by size, for too specific sets (<15 genes) or too general sets (>300 genes) to compare the control group versus each exposed group, using 1000 random permutations of the gene sets for resampling. A network analysis was performed to highlight dysregulated pathways using the Cytoscape software (version 3.8.2) (Cline et al., 2007) with the Enrichment Map plug-in (Merico et al., 2010). The selected gene sets with a False Discovery Ratio <0.05 (FDR), were represented with edges linking gene sets showing an overlap >30% and then clustered in function of their common biological functions.

Results

Experimental design

We exposed 3 groups of gestating mice from the inbred C57Bl6/J strain, which has a well-defined genetic background, to aerosols containing low concentration of either PQ (0.1 mg/m³), $nTiO_2$ (10 mg/m³) or PQ + $nTiO_2$ (10 mg/m³). These concentrations were selected for their relevance to human exposure (see methods for estimations). Aerosols exposure sessions were started at GD5, before the beginning of neurulation, to ensure a continuous exposure during the entire neurodevelopment. The last session was at GD18, i.e., 1.5 day before birth, to limit maternal stress during the perinatal period.

Pups were kept with their mother until PND14, a stage at which the main neurodevelopmental processes are completed. We then used an unbiased transcriptome analysis of gene expression of the post-natal striatum to highlight possible dysregulations caused by *in utero* exposures, and a possible cocktail effect. Following a previous study (Gollamudi et al., 2012), we selected this brain area for several reasons. It first represents a relatively homogenous and well delimitated brain area, where 95% of the neurons are GABAergic medium spiny neurons, known to be highly sensitive to moderate neurodevelopmental alterations (Richard et al., 2020). In addition, striatum neurons receive dopaminergic innervation from *subtantia nigra*, one of the main sites of the PQ neurotoxicity. Thus, we expected that the striatum gene expression could represent a sensitive endpoint to early neurodevelopmental insults.

Aerosol exposures and dosimetry assessment

The particle number concentrations assessed in real-time within the exposure chamber were stable over the duration of exposures for the three aerosols (Figure 1) and the results of particle number and mass concentrations are reported in Table 1. The average number

concentrations did not deviate from the mean by more than 9% and the mass concentrations matched the desired target concentrations with a maximum relative standard deviation of 8%.

The alveolar deposition fraction in gestating mice and human beings were calculated using the MPPD model to assess the alveolar deposited mass in each species (Table S2). For $nTiO_2$ and PQ, they were respectively 384 µg/m² and 229 µg/m² in human beings, and 298 µg/m² and 9 µg/m² in mice. Therefore, mice exposures during gestation resulted in an alveolar particle deposition below what a pregnant worker could theoretically be exposed to, if working during eight months at levels of exposure corresponding to the occupational exposure limit. The deposition fraction of the aerosol of PQ + $nTiO_2$ was estimated in a similar manner. Due to similar aerosol characteristics in terms of size distribution, no significant difference was found in its alveolar deposition in comparison with $nTiO_2$ alone in human being or mice. The mixture resulted in interactions between PQ and $nTiO_2$ particles in the aerosol phase, but the MMPD modelling cannot deconvolute the deposited mass attributable to each substance separately. Therefore, we were not able to decipher the deposition fraction in each substance (PQ versus $nTiO_2$) in the aerosol of PQ + $nTiO_2$.

General health endpoints of exposed females and litters

The treated mice did not display any obvious sign of discomfort. Statistical analysis did not evidence any significant effect of aerosol exposure on gestating mice weight gain, offspring survival, and litter body weights at different post-natal stages (Supplementary data, Figure S2)**.** In addition, prenatal aerosol exposures did not have any incidence on the characteristics of litters (number, sex ratio) or organ weight at PND14 (Table S3). Only two markers were detected in the plasma of pups (MMP12 and Cxcl1) (Figure 2). Cxcl1 chemokine was found to be slightly but significantly increased in the PQ group of exposure in comparison to the control group, which is an indication of a slight systemic inflammation in this group.

Assessing neurodevelopmental toxicity by transcriptome analysis

RNA was extracted from the striatum of pups at PND14 (Table S4). We first used RT-qPCR to address the possible accidental presence of neighboring neural tissues in the striatum samples. The expression of *Drd2* and *Adora2a*, whose expression is restricted to striatum, and *Fezf1* which is selectively expressed in the neighboring cortex, was homogeneous. Sixteen striatum samples (4/group, 50% males and 50% females) coming from sixteen different litters were selected for RNA-seq analysis. Deseq2 was then used to identify differentially expressed genes (DEGs) in each group of exposure in comparison to the control group. The Principal Component Analysis (PCA) of the total normalized counts (Figure 3A) highlighted different profiles for the different groups. The first principal component, explaining 37 % of the variation mainly reflected the groups exposure. The second principal component, explaining 26 % of the variation, mainly reflected the distinction between females and males. However, intragroup comparison between males and females did not evidence different response to aerosol exposures. Because of a hypothalamic contamination during dissection, one outlier coming from the PQ group was detected thanks to Deseq2 and excluded from the analysis.

Both PQ and $nTiO_2$ aerosols had a clear influence on gene expression. The number of differentially expressed genes (DEGs) was 2038 for PQ, 1249 for $nTiO_2$, and only 287 for PQ + $nTiO_2$. Up-regulation was more frequent that down-regulation (Figure 3B) as up-regulated genes represented 59%, 89% and 85% of the total number of DEGs for PQ, $nTiO_2$ and PQ + $nTiO_2$, and the fold-changes exceeded 1.5 for 120, 61 and 36 DEGs respectively. The overlapping DEGs between the three groups of exposure reached 170 (Figure 3C), suggesting that some similarities between the mode of action of PQ and $nTiO_2$. A smaller subset of 18 DEGs were upregulated in the three groups of exposure, with a fold-change superior to 1.5. In agreement with the previous global analysis, the combined exposure to PQ + $nTiO_2$ had globally a lesser influence on these 18 genes (Figure 3D).

RT-qPCR was used to confirm some of the RNA-seq observations on a larger number of animals for 8 genes selected for their known role in neurodevelopment (Figure 4). These genes were markers of neuronal differentiation (*Nefl, Nefh*) (Hogberg et al., 2009) reactive astrogliosis resulting from neurological insults (*Gfap*) (Eng and Ghirnikar, 1994) myelination (*Fa2h, Mobp*) (Royland et al., 2008; Potter et al., 2011) GABAergic neurons maturation (*Kcnc2*) (Fukumoto et al., 2018)and microglial activation (*Chga*) (Ciesielski-Treska and Aunis, 2000). *Bdnf* encodes a neutrophin, which is essential for the neuron survival, growth and differentiation, whose modification has been associated with mental disorders (Ikegame et al., 2013). The expression of *Nefl* and *Nefh*, which encode filament proteins expressed respectively during early and late neuronal maturation, were both found dysregulated in the PQ group, while only *Nefl* was found dysregulated in the PQ + $nTiO_2$ group. Interestingly, the expression of the *Chga* gene colocalizes with activated microglia in neurodegenerative areas (Ciesielski-Treska et al., 1998), was overexpressed in all exposure groups with the same amplitude. Moreover, *Kcnc2* which is highly expressed in the medium spiny neurons of striatum was clearly upregulated in the PQ and PQ + $nTiO_2$ groups. The expressions of *Gfap* and myelin-forming markers (*Fa2h* and *Mobp*) were upregulated solely in the PQ group. Overall, the dysregulation of these genes, with the possible exception of *Bdnf*, was more pronounced in the PQ group, supporting the observations coming from RNA-seq data.

Interpretation of transcriptome changes - Gene Set Enrichment Analysis

Gene Set Enrichment Analysis (GSEA) can identify differential expression of gene sets, when the expression difference between genes is minimal and cannot be evidence by classical methods on a single gene basis. GSEA was used to interpret the broad but often modest changes in gene expression revealed by RNA-seq, to identify relevant biological pathways. Overall, 77 gene sets were found dysregulated in the striatum of at least one group of mice (Supplementary Tables S5 to S7).

PQ exposure resulted in the up-regulation of 7 gene sets involved in gliogenesis and axon ensheathment, and 4 gene sets associated with neuron projection and axon guidance (Figure 5A). This suggested an alteration in the timing of differentiation for both oligodendrocytes and the main neuronal cell type, the medium spiny neurons. Among the five identified pathways which were down-regulated, two were likely to reflect a possible direct effect and persisting of PQ in the post-natal brain, following fetal contamination, as they are known to be involved in the etiology of the PD. These are related to redox homeostasis (1 gene set) and mitochondrial electron transport (8 genes sets), which may be linked to PQ oxidant properties. The subset of genes accounting for the enrichment of this pathway, the leading-edge genes according to GSEA results, was analyzed using ClueGO (version 2.5.7) (Bindea et al., 2009)from the Cytoscape package in order to visualize the deregulated pathways in a functionally grouped gene network. A focus presenting the 53 leading edge genes of Parkinson disease gene set (KEGG, total of 110 genes) is presented in Figure 5B, showing that 32 of them were specifically related to the oxidative phosphorylation pathway. In addition, the gene set associated with the cell redox homeostasis (total of 52 genes) encompassed 24 leading edge genes. Within this set, 18 genes were related to the oxidoreductase activity, involving for example the Glutathione reductase (*Gsr*), which is necessary to maintain high levels of reduced glutathione in the cytosol (Yang et al., 2006).

The consequences of gestational exposure to $nTiO_2$ were also highlighted (Figure 5A), with only one down-regulated pathway (centromere complex assembly, 2 gene sets), and 4 up-regulated pathways. These pathways were related to gliogenesis, axon ensheathment and guidance (5 gene sets). This is an indication that $nTiO_2$ also may have adverse effects on oligodendrocytes differentiation and neuronal maturation. The identification of the ion homeostasis pathway (5 gene sets) also suggested an alteration of the neuronal electrophysiology. The appearance of the pathway “Chemokines production and B-Cell

proliferation" pointed out a potential low grade neuroinflammation. Finally, $nTiO_2$ exposure also altered the "regulation of neurotransmitters" pathway (11 gene sets).

The gestational exposure to the combination of PQ + $nTiO_2$ had a visible influence on only 3 pathways (Figure 5A) which is consistent with its decreased influence on the gene expression. These pathways are: "regulation of neurotransmitters" (12 gene sets), "neurons and dendrites extension" (2 gene sets) and "voltage potassium channels" (4 gene sets). As the regulation of neurotransmitters was commonly found upregulated only in the $nTiO_2$ and PQ + $nTiO_2$ groups, the dysregulation of genes involved in neurotransmitters release is probably caused by $nTiO_2$, independently of PQ. The first 50 leading edge genes accounting for the enrichment of this pathway were represented using ClueGO (Figure 5B). These common genes accounting for the enrichment of this pathway and their associated fold-changes were represented on a radar plot for the $nTiO_2$ and PQ + $nTiO_2$ groups, showing a similar influence of both exposures (Figure S4). This demonstrated that PQ + $nTiO_2$ did not have an additive effect on this pathway, which is dysregulated by both $nTiO_2$ and the mixture. Interestingly, two genes related to the glutamate neurotransmission were highlighted: the Glutamate receptor (*Grina3*) and the Metabotropic glutamate receptor 4 (*Grm4*). α-synuclein was also found in the leading edge set of this pathway and different trends were observed, as a slight decrease was found after exposure to PQ (Fold-change=0.80, adjusted p-value=0.01) and $nTiO_2$ (Fold-change=0.82, adjusted p-value=0.02), but not to PQ + $nTiO_2$.

Discussion

Effect of maternal exposure to aerosols

We present novel evidence showing that prenatal exposures to aerosols of PQ and/or $nTiO_2$ at low concentrations, which are theoretically considered safe, have a significant effect on the

gene expression in the developing brain . The calculation of the deposition fractions for each aerosol using dosimetry modeling allowed an interspecies extrapolation. We could identify some consequences of the *in utero* exposure by analyzing the gene expression in the post-natal striatum. In this context, transcriptome analysis proved to be an unbiased, powerful and sensitive method to detect neurodevelopmental alterations.

Paraquat neurodevelopmental toxicity

Despite a very low deposition of PQ in maternal lungs, clear changes in gene expression were observed in the striatum of pups after birth, irrespective of the gender, which reflect alterations in different cell lineages. The observed changes suggest moderate defects in neuronal maturation and oligodendrocytes differentiation. They are also indicative of inflammation, with astrogliosis and microglial cells activation. Therefore, the influence of PQ in the developing striatum is not limited to dopaminergic neurons and we propose that it combines direct and indirect effects on neural cells. Based on previous toxicological knowledge and our observations, PQ may directly alter the mitochondrial function and the redox status in neurons, during fetal and early post-natal life, as it does in adult brain to induce Parkinson disease (Jomova et al., 2010). Some of the highlighted changes in gene expression are possibly involved in this process: Glutathione reductase (encoded by the *Gsr* gene) is necessary to maintain high levels of reduced glutathione in the cytosol (Yang et al., 2006), Selenoprotein (product of the *Selenot* gene) protects dopaminergic neurons against oxidative stress in mouse models of Parkinson disease (Boukhzar et al., 2016), Parkin RBR E3 ubiquitin protein ligase (*Prkn*), and α-synuclein (*Snca*) maintain the dopamine neuronal homeostasis, whose dysfunction is related to the onset of Parkinson disease (Kuroda et al., 2012; Oczkowska et al., 2013). These initial mitochondrial alterations may indirectly influence the maturation of the neuronal networks, the post-natal myelination process, and eventually favor neuroinflammation. Taken together, these observations suggest that PQ alters

mitochondrial functions in the striatum of exposed pups in a way that is reminiscent of the pathological process leading to Parkinson disease.

This interpretation is consistent with an analysis of the striatum transcriptome performed after acute exposure of adult mice to PQ (Gollamudi et al., 2012). This also caused dysregulations of the signaling pathways related to Parkinson disease. Exposure of gestating mice to a high dose of PQ via the oral route (Ait-Bali et al., 2016) also induced various neurological and behavioral alterations in the offspring. In a recent study, adult C57Bl/6J mice were exposed to PQ aerosols (Anderson et al., 2021), leading to a significant PQ burden in different brain regions, including the striatum, associated with a male-specific deficit in olfaction, which is part of the prodromal features of Parkinson disease.

The amplitude of the observed changes is modest but does not rule out unforeseen latter consequences, as early alterations can exacerbate the sensitivity to additional stressors at adult stage (Barouki et al., 2012). Previous analysis also showed that early exposure to PQ + Zn in rats affects the oxidative stress, inflammation, cell death, dopamine metabolism and storage regulating machineries (Mittra et al., 2020). Therefore, re-exposure of adult rats caused more pronounced changes in all the observed endpoints of toxicity, compared with rat exposed only during adulthood, thereby showing that early insults emphasized the toxicity of secondary exposures. Similar conclusions were drawn for the early exposure to PQ combined with maneb (Colle et al., 2020).

$nTiO_2$ neurodevelopmental toxicity

The neurotoxicity of $nTiO_2$ was previously addressed at higher concentrations than those used here. Subcutaneous injection of large quantities of $nTiO_2$ to gestating mice induces a mitochondrial respiration dysfunction in the pups brain (Hathaway et al., 2017) altering the gene expression in the post-natal striatum of pups (Umezawa et al., 2012) and having long term consequences on their cognitive functions (Engler-Chiurazzi et al., 2016). Prenatal

exposure to $nTiO_2$ aerosols also results in maternal and fetal microvascular dysfunction (Stapleton et al., 2015) and affects theproduction of neurotransmitters (Shimizu et al., 2009). Our results confirm that gestational exposure to $nTiO_2$ has adverse effect on striatum maturation, at a concentration, which is much lower than those used in previous studies. Changes in gene expression suggest a modulation of neuronal maturation, neurotransmitter production, post-natal myelination, and possibly a low-grade neuro-inflammation. The convergence of our conclusions with previous studies suggests that the observed changes are neither transient nor adaptative but rather reflects moderate adverse effects on the brain maturation. The possibility that exposure to aerosols containing realistic concentrations of $nTiO_2$ could compromise the neurodevelopment should thus be a matter of concern when considering their extensive use.

Interaction between $nTiO_2$ *and PQ exposure.*

We did not observe a synergistic nor an additive effect when combining PQ and $nTiO_2$. Instead, their association in aerosol phase seemed to lessen the effect of each substance. RNA-seq and RT-qPCR showed that the number of differentially expressed genes and the amplitude of the changes in gene expression were globally lower compared to pups exposed to either PQ or $nTiO_2$ solely. Moreover, unlike the PQ group, the concentration of the Cxcl1 inflammation marker was not increased in the pups plasma. The reduction of the mixture effect is not due to the PQ degradation by $nTiO_2$, as verified previously (Hamdaoui et al., 2021) but might reflect interactions between PQ and $nTiO_2$ particles. The aerosols of $nTiO_2$ and PQ + $nTiO_2$ presented very similar particle size distributions, and the mixture displayed number concentrations that did not correspond to the sum of the reported concentrations for PQ and $nTiO_2$ taken separately. These elements suggest that mixing these substances prior to the aerosol generation does not produce two distinct populations of particles, but rather a composite population of particles associating PQ and $nTiO_2$. As PQ can be adsorbed on $nTiO_2$

in suspension (Vohra and Tanaka, 2003; Florencio et al., 2004; Phuinthiang and Kajitvichyanukul, 2019) these interactions are likely to occur during the nebulization process and in the aerosol phase. We hypothesize that this sorption changes the deposition fraction, biodistribution and particle toxicokinetics in a way which remains to be addressed. While PQ is suspected to cross the placental barrier (Ingebrigtsen et al., 1984) sorption to $nTiO_2$ might prevent this translocation. It has been shown previously that $nTiO_2$ caused a retention of the Cd^{2+} ions, thereby decreasing their bioavailability and preventing ecotoxicological effects. Eventually, $nTiO_2$ might have the same effect on the PQ toxic forms (PQ^{2+}/PQ^{+}), by decreasing its bioavailability and therefore its toxicity. *Limitations of the present study*

We generated ultrafine PQ particles that do not strictly correspond to the primary size of sprayed pesticide particles in agriculture, which are rather coarse particles (>10 µm) mostly considered as not inhalable (Chester and Ward, 1984). Nevertheless, according to its long environmental persistence and the wind erosion of soil particles containing PQ, occupational or residential populations can be exposed to inhalable PQ particles. This is in line with a size range of 0.1 - 1 µm measured for airborne residue of some pesticides (Coscollo et al., 2013). Secondary exposure to pesticide residues therefore encompass particles that may be deposited in the airways after their atmospheric transport.

We studied the consequences of gestational exposures to PQ and $nTiO_2$ aerosols at a single time-point in the striatum, which does not allow to address the reversibility of the observed changes. Also, in the absence of complementary histological, biochemical and behavioral analysis, the interpretation of these changes remains hypothetical. Finally, further work would be needed to clarify the mechanisms by which the combination of PQ and $nTiO_2$ seems to lower their inhalation effects, and whether this conclusion would also apply to other cocktails of substances potentially suitable for nanopesticide formulation.

Conclusions

This study demonstrates the pertinence to use an aerosol exposure chamber and RNA-seq analysis to better evaluate the unknown effects of low and repeated exposures to nanopesticide aerosols on neurodevelopment. Considering the growing demand for these innovative products and the lack of precise guidelines surrounding their health risk assessment, these results should reinforce awareness about their future sanitary impact. Taken together, these data also suggest that the risk associated with the exposure of aerosols containing PQ or $nTiO_2$ during critical stages, like pregnancy and early development, may have been previously underestimated.

Acknowledgements

We thank Benjamin Gillet and Sandrine Hughes from the IGFL-PSI facility for deep sequencing, and the Plateau de Biologie Expérimentale de la Souris (SFR Biosciences UAR3444) for mouse breeding. This work was carried out as part of a thesis supported by a CIFRE fellowship involving the collaboration of the LNE and the École Normale Supérieure de Lyon (ENS de Lyon), by the ANSES (Thyrogenox program, PNRPE Ecophyto II) and the European Union's Horizon 2020 research and innovation program under grant agreement N°825753 (ERGO).

Authors contribution.

QH conceived the aerosol exposure device, performed the experiments, the data analysis, the tissue collection and wrote the manuscript, YZ performed data analysis, SR, DA, RG, SM and KG participated to mouse breeding and tissue collection. FGL conceived the aerosol exposure device. AB conceived and supervised the experiments, FF supervised the project and wrote the manuscript. All authors reviewed and edited the manuscript.

Figure legends

Figure 1. Real time measurement of aerosol particle number concentration in the chamber during animal exposures.

Data are presented as means ± standard deviation (SD) for each aerosol.

Figure 2. Plasmatic Markers of inflammation in pups (PND14) exposed in utero.

Two out of 8 assessed cytokines were detectable by ELISA. No changes were detected in MMP12 expression in any of the exposure groups. The Cxcl1 expression is similar between control and pups exposed to $nTiO_2$ alone or associated to PQ alone. PQ exposures caused a significant increase in Cxcl1 in comparison to the control group ($n \geq 5$/litter, * p-value <0.05), thereby suggesting a low grade inflammation. Comparisons between groups were performed with the Kruskal-Wallis test (nonparametric test), followed by multiple mean comparisons with Dunn's test. Data presented as means ± SEM.

Figure 3. Transcriptome analysis of pups striatum. (A) PCA of the gene expression in 15 pups. (B) Volcano plots summarizing the comparisons between the groups of exposure versus the control group. (C) Venn diagram showing the overlap between DEGs for the 3 exposed groups (adjusted p-value <0.05; no threshold on fold-change), a main part of genes is associated with the PQ exposure only, $nTiO_2$ shared 68% of its DEGs with PQ, PQ + $nTiO_2$ shared 81% with PQ and 65% with $nTiO_2$. (E) Fold-changes of the 18 DEGs up-regulated in the 3 groups with a fold-change >1.5; note that the response to the PQ + $nTiO_2$ is always equal or lower than the response to the single substances.

Figure 4. RT-qPCR analysis of gene expression in pups striatum at PND14.

Comparisons between groups ($N \geq 8$ for each group, 50% females and 50% males coming from at least 4 different litters) were performed with the Kruskal-Wallis test, followed by

multiple mean comparisons with Dunn's test. * $p<0.05$ **$p<0.01$. Data presented as means ± SEM.

Figure 5. Gene Set Enrichment Analysis of striatum gene expression profiles.

(A) Three MSigDB genes collections were analyzed: Gene Ontology (GO) Biological Process ontology and two Canonical Pathways gene sets derived from the KEGG pathway database and from the Reactome pathway database. Each node represents a gene set significantly enriched in comparison with controls. The gene sets corresponding to each node, can be found in supplementary data (Figure S3). Nodes are clustered in pathways based on their shared genes and their common biological functions. Edges are filtered with an overlap cutoff: the minimum edge between two nodes depict that 35% of one gene set is common with the other (B) ClueGO analysis of the leading-edge gene set associated with KEGG Parkinson disease in the PQ group, represented to highlight the main biological function associated with those, notably the oxidative phosphorylation. (C) ClueGO analysis of the leading-edge gene set associated with the GO regulation of neurotransmitter levels in the $nTiO_2$ and PQ+$nTiO_2$ groups.

References

Agathokleous, E., Feng, Z.Z., Iavicoli, I., Calabrese, E.J., 2020. Nano-pesticides: A great challenge for biodiversity? The need for a broader perspective. Nano Today 30, 100808-100810.

Ait-Bali, Y., Ba-M'hamed, S., Bennis, M., 2016. Prenatal Paraquat exposure induces neurobehavioral and cognitive changes in mice offspring. Environ Toxicol Pharmacol 48, 53-62.

Anders, S., Pyl, P.T., Huber, W., 2015. HTSeq--a Python framework to work with high-throughput sequencing data. Bioinformatics 31, 166-169.

Anderson, T., Merrill, A.K., Eckard, M.L., Marvin, E., Conrad, K., Welle, K., Oberdorster, G., Sobolewski, M., Cory-Slechta, D.A., 2021. Paraquat Inhalation, a Translationally Relevant Route of Exposure: Disposition to the Brain and Male-Specific Olfactory Impairment in Mice. Toxicol Sci 180, 175-185.

Barouki, R., Gluckman, P.D., Grandjean, P., Hanson, M., Heindel, J.J., 2012. Developmental origins of non-communicable disease: implications for research and public health. Environ Health 11, 42.

Bencsik, A., Lestaevel, P., Guseva Canu, I., 2018. Nano- and neurotoxicology: An emerging discipline. Prog Neurobiol 160, 45-63.

Bindea, G., Mlecnik, B., Hackl, H., Charoentong, P., Tosolini, M., Kirilovsky, A., Fridman, W.H., Pages, F., Trajanoski, Z., Galon, J., 2009. ClueGO: a Cytoscape plug-in to decipher functionally grouped gene ontology and pathway annotation networks. Bioinformatics 25, 1091-1093.

Bongaerts, E., Nawrot, T.S., Van Pee, T., Ameloot, M., Bove, H., 2020. Translocation of (ultra)fine particles and nanoparticles across the placenta; a systematic review on the evidence of in vitro, ex vivo, and in vivo studies. Part Fibre Toxicol 17, 56.

Boukhzar, L., Hamieh, A., Cartier, D., Tanguy, Y., Alsharif, I., Castex, M., Arabo, A., El Hajji, S., Bonnet, J.J., Errami, M., Falluel-Morel, A., Chagraoui, A., Lihrmann, I., Anouar, Y., 2016. Selenoprotein T Exerts an Essential Oxidoreductase Activity That Protects Dopaminergic Neurons in Mouse Models of Parkinson's Disease. Antioxid Redox Signal 24, 557-574.

Boyes, W.K., van Thriel, C., 2020. Neurotoxicology of Nanomaterials. Chem Res Toxicol 33, 1121-1144.

Brouwer, M., Huss, A., van der Mark, M., Nijssen, P.C.G., Mulleners, W.M., Sas, A.M.G., van Laar, T., de Snoo, G.R., Kromhout, H., Vermeulen, R.C.H., 2017. Environmental exposure to pesticides and the risk of Parkinson's disease in the Netherlands. Environ Int 107, 100-110.

Cassee, F., de Winter-Sorkina, R., 2003. From concentration to dose: Factors influencing airborne particulate matter deposition in humans and the rat human dose extrapolation. Toxicological Sciences 72, 39-39.

Cena, V., Jativa, P., 2018. Nanoparticle crossing of blood-brain barrier: a road to new therapeutic approaches to central nervous system diseases. Nanomedicine (Lond) 13, 1513-1516.

Chester, G., Ward, R.J., 1984. Occupational exposure and drift hazard during aerial application of paraquat to cotton. Arch Environ Contam Toxicol 13, 551-563.

Ciesielski-Treska, J., Aunis, D., 2000. Chromogranin A induces a neurotoxic phenotype in brain microglial cells. Adv Exp Med Biol 482, 291-298.

Ciesielski-Treska, J., Ulrich, G., Taupenot, L., Chasserot-Golaz, S., Corti, A., Aunis, D., Bader, M.F., 1998. Chromogranin A induces a neurotoxic phenotype in brain microglial cells. J Biol Chem 273, 14339-14346.

Cline, M.S., Smoot, M., Cerami, E., Kuchinsky, A., Landys, N., Workman, C., Christmas, R., Avila-Campilo, I., Creech, M., Gross, B., Hanspers, K., Isserlin, R., Kelley, R., Killcoyne, S., Lotia, S., Maere, S., Morris, J., Ono, K., Pavlovic, V., Pico, A.R., Vailaya, A., Wang, P.L., Adler, A., Conklin, B.R., Hood, L., Kuiper, M., Sander, C., Schmulevich, I., Schwikowski, B., Warner, G.J., Ideker, T., Bader, G.D., 2007. Integration of biological networks and gene expression data using Cytoscape. Nat Protoc 2, 2366-2382.

Colle, D., Santos, D.B., Naime, A.A., Goncalves, C.L., Ghizoni, H., Hort, M.A., Farina, M., 2020. Early Postnatal Exposure to Paraquat and Maneb in Mice Increases Nigrostriatal Dopaminergic Susceptibility to a Re-challenge with the Same Pesticides at Adulthood: Implications for Parkinson's Disease. Neurotox Res 37, 210-226.

Coscollo, C., Yahyaoui, A., Colin, P., Robin, C., Martinon, L., Val, S., Baeza-Squiban, A., Mellouki, A., Yusa, V., 2013. Particle size distributions of currently used pesticides in a rural atmosphere of France. Atmos Environ 81, 32-38.

Cui, Y., Chen, X., Zhou, Z., Lei, Y., Ma, M., Cao, R., Sun, T., Xu, J., Huo, M., Cao, R., Wen, C., Che, Y., 2014. Prenatal exposure to nanoparticulate titanium dioxide enhances depressive-like behaviors in adult rats. Chemosphere 96, 99-104.

Eng, L.F., Ghirnikar, R.S., 1994. GFAP and astrogliosis. Brain Pathol 4, 229-237.

Engler-Chiurazzi, E.B., Stapleton, P.A., Stalnaker, J.J., Ren, X., Hu, H., Nurkiewicz, T.R., McBride, C.R., Yi, J., Engels, K., Simpkins, J.W., 2016. Impacts of prenatal nanomaterial exposure on male adult Sprague-Dawley rat behavior and cognition. J Toxicol Environ Health A 79, 447-452.

Florencio, M.H., Pires, E., Castro, A.L., Nunes, M.R., Borges, C., Costa, F.M., 2004. Photodegradation of Diquat and Paraquat in aqueous solutions by titanium dioxide: evolution of degradation reactions and characterisation of intermediates. Chemosphere 55, 345-355.

585 Fukumoto, K., Tamada, K., Toya, T., Nishino, T., Yanagawa, Y., Takumi, T., 2018.
586 Identification of genes regulating GABAergic interneuron maturation. Neurosci Res 134, 18-
587 29.

588 Gilbertson, L.M., Pourzahedi, L., Laughton, S., Gao, X.Y., Zimmerman, J.B., Theis, T.L.,
589 Westerhoff, P., Lowry, G.V., 2020. Guiding the design space for nanotechnology to advance
590 sustainable crop production. Nat Nanotechnol 15, 801-+.

591 Gollamudi, S., Johri, A., Calingasan, N.Y., Yang, L., Elemento, O., Beal, M.F., 2012.
592 Concordant signaling pathways produced by pesticide exposure in mice correspond to
593 pathways identified in human Parkinson's disease. PLoS One 7, e36191.

594 Guillard, A., Gaultier, E., Cartier, C., Devoille, L., Noireaux, J., Chevalier, L., Morin, M.,
595 Grandin, F., Lacroix, M.Z., Comera, C., Cazanave, A., de Place, A., Gayrard, V., Bach, V.,
596 Chardon, K., Bekhti, N., Adel-Patient, K., Vayssiere, C., Fisicaro, P., Feltin, N., de la Farge,
597 F., Picard-Hagen, N., Lamas, B., Houdeau, E., 2020. Basal Ti level in the human placenta and
598 meconium and evidence of a materno-foetal transfer of food-grade TiO(2)nanoparticles in an
599 ex vivo placental perfusion model. Particle and Fibre Toxicology 17.

600 Hamdaoui, Q., Bencsik, A., Flamant, F., Delcour , S., Macé, T., Vaslin-Reimann, S., Gaie-
601 Levrel, F., 2021. Development and characterization of an aerosol exposure chamber to
602 explore the nanopesticides inhalation effects on rodents Aerosol and Air Quality Research in
603 press.

604 Hathaway, Q.A., Nichols, C.E., Shepherd, D.L., Stapleton, P.A., McLaughlin, S.L.,
605 Stricker, J.C., Rellick, S.L., Pinti, M.V., Abukabda, A.B., McBride, C.R., Yi, J., Stine, S.M.,
606 Nurkiewicz, T.R., Hollander, J.M., 2017. Maternal-engineered nanomaterial exposure disrupts
607 progeny cardiac function and bioenergetics. Am J Physiol Heart Circ Physiol 312, H446-
608 H458.

609 Hogberg, H.T., Kinsner-Ovaskainen, A., Hartung, T., Coecke, S., Bal-Price, A.K., 2009.
610 Gene expression as a sensitive endpoint to evaluate cell differentiation and maturation of the
611 developing central nervous system in primary cultures of rat cerebellar granule cells (CGCs)
612 exposed to pesticides. Toxicol Appl Pharm 235, 268-286.
613 Ikegame, T., Bundo, M., Murata, Y., Kasai, K., Kato, T., Iwamoto, K., 2013. DNA
614 methylation of the BDNF gene and its relevance to psychiatric disorders. J Hum Genet 58,
615 434-438.
616 Ingebrigtsen, K., Nafstad, I., Andersen, R.A., 1984. Distribution and transplacental transfer
617 of paraquat in rats and guinea-pigs. Gen Pharmacol 15, 201-204.
618 Jarabek, A.M., Asgharian, B., Miller, F.J., 2005. Dosimetric adjustments for interspecies
619 extrapolation of inhaled poorly soluble particles (PSP). Inhal Toxicol 17, 317-334.
620 Jomova, K., Vondrakova, D., Lawson, M., Valko, M., 2010. Metals, oxidative stress and
621 neurodegenerative disorders. Mol Cell Biochem 345, 91-104.
622 Kah, M., Kookana, R.S., Gogos, A., Bucheli, T.D., 2018. A critical evaluation of
623 nanopesticides and nanofertilizers against their conventional analogues. Nat Nanotechnol 13,
624 677-684.
625 Kah, M., Tufenkji, N., White, J.C., 2019. Nano-enabled strategies to enhance crop
626 nutrition and protection. Nat Nanotechnol 14, 532-540.
627 Kamel, F., Tanner, C.M., Umbach, D.M., Hoppin, J.A., Alavanja, M.C.R., Blair, A.,
628 Comyns, K., Goldman, S.M., Korell, M., Langston, J.W., Ross, G.W., Sandler, D.P., 2007.
629 Pesticide exposure and self-reported Parkinson's disease in the agricultural health study. Am J
630 Epidemiol 165, 364-374.
631 Kookana, R.S., Boxall, A.B., Reeves, P.T., Ashauer, R., Beulke, S., Chaudhry, Q.,
632 Cornelis, G., Fernandes, T.F., Gan, J., Kah, M., Lynch, I., Ranville, J., Sinclair, C., Spurgeon,

633 D., Tiede, K., Van den Brink, P.J., 2014. Nanopesticides: guiding principles for regulatory
634 evaluation of environmental risks. J Agric Food Chem 62, 4227-4240.
635 Kuroda, Y., Sako, W., Goto, S., Sawada, T., Uchida, D., Izumi, Y., Takahashi, T.,
636 Kagawa, N., Matsumoto, M., Matsumoto, M., Takahashi, R., Kaji, R., Mitsui, T., 2012.
637 Parkin interacts with Klokin1 for mitochondrial import and maintenance of membrane
638 potential. Hum Mol Genet 21, 991-1003.
639 Lee, J.H., Kwon, M., Ji, J.H., Kang, C.S., Ahn, K.H., Han, J.H., Yu, I.J., 2011. Exposure
640 assessment of workplaces manufacturing nanosized TiO2 and silver. Inhal Toxicol 23, 226-
641 236.
642 Livak, J.L., Schmittgen, T.D., 2001. Analysis of relative gene expression data using real-
643 time quantitative PCR and the 2-DDCT method. Methods 25, 402-408.
644 Love, M.I., Anders, S., Kim, V., Huber, W., 2015. RNA-Seq workflow: gene-level
645 exploratory analysis and differential expression. F1000Res 4, 1070.
646 Merico, D., Isserlin, R., Stueker, O., Emili, A., Bader, G.D., 2010. Enrichment Map: A
647 Network-Based Method for Gene-Set Enrichment Visualization and Interpretation. Plos One
648 5.
649 Mittra, N., Chauhan, A.K., Singh, G., Patel, D.K., Singh, C., 2020. Postnatal zinc or
650 paraquat administration increases paraquat or zinc-induced loss of dopaminergic neurons:
651 insight into augmented neurodegeneration. Mol Cell Biochem 467, 27-43.
652 Moisan, F., Spinosi, J., Delabre, L., Gourlet, V., Mazurie, J.L., Benatru, I., Goldberg, M.,
653 Weisskopf, M.G., Imbernon, E., Tzourio, C., Elbaz, A., 2015. Association of Parkinson's
654 Disease and Its Subtypes with Agricultural Pesticide Exposures in Men: A Case-Control
655 Study in France. Environ Health Persp 123, 1123-1129.
656 Mooney, M.A., Wilmot, B., 2015. Gene set analysis: A step-by-step guide. Am J Med
657 Genet B Neuropsychiatr Genet 168, 517-527.

Morshed, M.M., Omar, D., Mohamad, R., Wahed, S., Rahman, M.A., 2010. Airborne Paraquat Measurement and its Exposure to Spray Operators in Treated Field Environment. Int J Agric Biol 12, 679-684.

Naasz, S., Altenburger, R., Kuhnel, D., 2018. Environmental mixtures of nanomaterials and chemicals: The Trojan-horse phenomenon and its relevance for ecotoxicity. Sci Total Environ 635, 1170-1181.

Nicosia, A., Vento, F., Di Mari, G.M., D'Urso, L., Mineo, P.G., 2021. TiO2-Based Nanocomposites Thin Film Having Boosted Photocatalytic Activity for Xenobiotics Water Pollution Remediation. Nanomaterials-Basel 11.

Nishimori, H., Kondoh, M., Isoda, K., Tsunoda, S., Tsutsumi, Y., Yagi, K., 2009. Influence of 70 nm silica particles in mice with cisplatin or paraquat-induced toxicity. Pharmazie 64, 395-397.

Nist, M.D., Pickler, R.H., 2019. An Integrative Review of Cytokine/Chemokine Predictors of Neurodevelopment in Preterm Infants. Biol Res Nurs 21, 366-376.

Oczkowska, A., Kozubski, W., Lianeri, M., Dorszewska, J., 2013. Mutations in PRKN and SNCA Genes Important for the Progress of Parkinson's Disease. Curr Genomics 14, 502-517.

Phuinthiang, P., Kajitvichyanukul, P., 2019. Degradation of paraquat from contaminated water using green TiO2 nanoparticles synthesized from Coffea arabica L. in photocatalytic process. Water Sci Technol 79, 905-910.

Pimentel, D., 2014. Pesticides Applied for the Control of Invasive Species in the United States. Integrated Pest Management: Current Concepts and Ecological Perspective, 111-123.

Potter, K.A., Kern, M.J., Fullbright, G., Bielawski, J., Scherer, S.S., Yum, S.W., Li, J.J., Cheng, H., Han, X., Venkata, J.K., Khan, P.A., Rohrer, B., Hama, H., 2011. Central nervous system dysfunction in a mouse model of FA2H deficiency. Glia 59, 1009-1021.

682 Richard, S., Guyot, R., Rey-Millet, M., Prieux, M., Markossian, S., Aubert, D., Flamant,
683 F., 2020. A Pivotal Genetic Program Controlled by Thyroid Hormone during the Maturation
684 of GABAergic Neurons. iScience 23, 100899.
685 Royland, J.E., Parker, J.S., Gilbert, M.E., 2008. A genomic analysis of subclinical
686 hypothyroidism in hippocampus and neocortex of the developing rat brain. J Neuroendocrinol
687 20, 1319-1338.
688 Sartori, F., Vidrio, E., 2018. Environmental fate and ecotoxicology of paraquat: a
689 California perspective. Toxicol Environ Chem 100, 479-517.
690 Schummer, C., Mothiron, E., Appenzeller, B.M.R., Wennig, R., Millet, M., 2010.
691 Gas/particle partitioning of currently used pesticides in the atmosphere of Strasbourg
692 (France). Air Qual Atmos Hlth 3, 171-181.
693 Shi, H.B., Magaye, R., Castranova, V., Zhao, J.S., 2013. Titanium dioxide nanoparticles: a
694 review of current toxicological data. Particle and Fibre Toxicology 10.
695 Shimizu, M., Tainaka, H., Oba, T., Mizuo, K., Umezawa, M., Takeda, K., 2009. Maternal
696 exposure to nanoparticulate titanium dioxide during the prenatal period alters gene expression
697 related to brain development in the mouse. Particle and Fibre Toxicology 6.
698 Stapleton, P.A., McBride, C.R., Yi, J., Nurkiewicz, T.R., 2015. Uterine microvascular
699 sensitivity to nanomaterial inhalation: An in vivo assessment. Toxicol Appl Pharmacol 288,
700 420-428.
701 Stone, K.C., Mercer, R.R., Gehr, P., Stockstill, B., Crapo, J.D., 1992. Allometric
702 Relationships of Cell Numbers and Size in the Mammalian Lung. Am J Resp Cell Mol 6, 235-
703 243.
704 Subramanian, A., Tamayo, P., Mootha, V.K., Mukherjee, S., Ebert, B.L., Gillette, M.A.,
705 Paulovich, A., Pomeroy, S.L., Golub, T.R., Lander, E.S., Mesirov, J.P., 2005. Gene set

706 enrichment analysis: a knowledge-based approach for interpreting genome-wide expression
707 profiles. Proc Natl Acad Sci U S A 102, 15545-15550.

708 Sun, Y., Liang, J., Tang, L., Li, H., Zhu, Y., Jiang, D.N., Song, B., Chen, M., Zeng, G.M.,
709 2019. Nano-pesticides: A great challenge for biodiversity? Nano Today 28.

710 Takahashi, Y., Mizuo, K., Shinkai, Y., Oshio, S., Takeda, K., 2010. Prenatal exposure to
711 titanium dioxide nanoparticles increases dopamine levels in the prefrontal cotex and
712 neostriatum of mice. J Toxicol Sci 35, 749-756.

713 Tamayo, P., Steinhardt, G., Liberzon, A., Mesirov, J.P., 2016. The limitations of simple
714 gene set enrichment analysis assuming gene independence. Stat Methods Med Res 25, 472-
715 487.

716 Tankersley, C.G., Fitzgerald, R.S., Kleeberger, S.R., 1994. Differential Control of
717 Ventilation among Inbred Strains of Mice. Am J Physiol-Reg I 267, R1371-R1377.

718 Tanner, C.M., Kamel, F., Ross, G.W., Hoppin, J.A., Goldman, S.M., Korell, M., Marras,
719 C., Bhudhikanok, G.S., Kasten, M., Chade, A.R., Comyns, K., Richards, M.B., Meng, C.,
720 Priestley, B., Fernandez, H.H., Cambi, F., Umbach, D.M., Blair, A., Sandler, D.P., Langston,
721 J.W., 2011. Rotenone, Paraquat, and Parkinson's Disease. Environ Health Persp 119, 866-872.

722 Tomita, M., Okuyama, T., Katsuyama, H., Miura, Y., Nishimura, Y., Hidaka, K., Otsuki,
723 T., Ishikawa, T., 2007. Mouse model of paraquat-poisoned lungs and its gene expression
724 profile. Toxicology 231, 200-209.

725 Umezawa, M., Tainaka, H., Kawashima, N., Shimizu, M., Takeda, K., 2012. Effect of fetal
726 exposure to titanium dioxide nanoparticle on brain development - brain region information. J
727 Toxicol Sci 37, 1247-1252.

728 Vohra, M.S., Tanaka, K., 2003. Photocatalytic degradation of aqueous pollutants using
729 silica-modified TiO2. Water Res 37, 3992-3996.

730 Wang, A., Costello, S., Cockburn, M., Zhang, X.B., Bronstein, J., Ritz, B., 2011.
731 Parkinson's disease risk from ambient exposure to pesticides. Eur J Epidemiol 26, 547-555.
732 Wang, Y., Sun, C., Zhao, X., Cui, B., Zeng, Z., Wang, A., Liu, G., Cui, H., 2016. The
733 Application of Nano-TiO2 Photo Semiconductors in Agriculture. Nanoscale Res Lett 11, 529.
734 Yang, M.S., Chan, H.W., Yu, L.C., 2006. Glutathione peroxidase and glutathione
735 reductase activities are partially responsible for determining the susceptibility of cells to
736 oxidative stress. Toxicology 226, 126-130.
737 Zhang, X.C., Li, W., Yang, Z., 2015. Toxicology of nanosized titanium dioxide: an update.
738 Archives of Toxicology 89, 2207-2217.

739

A

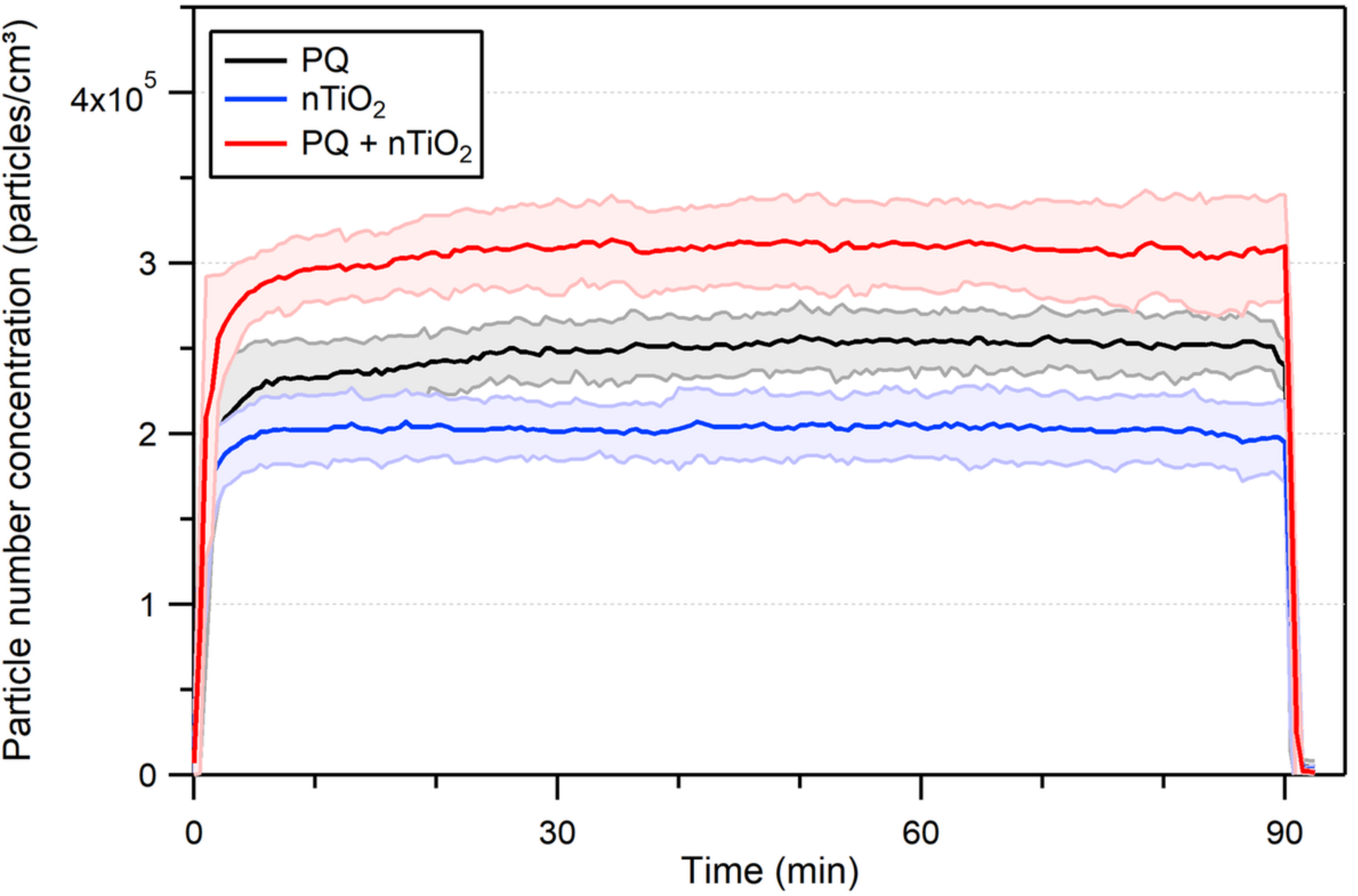
PQ
nTiO2
PQ + nTiO2
4x10^5
3
2
1
0
Particle number concentration (particles/cm³)
0
30
60
90
Time (min)

B

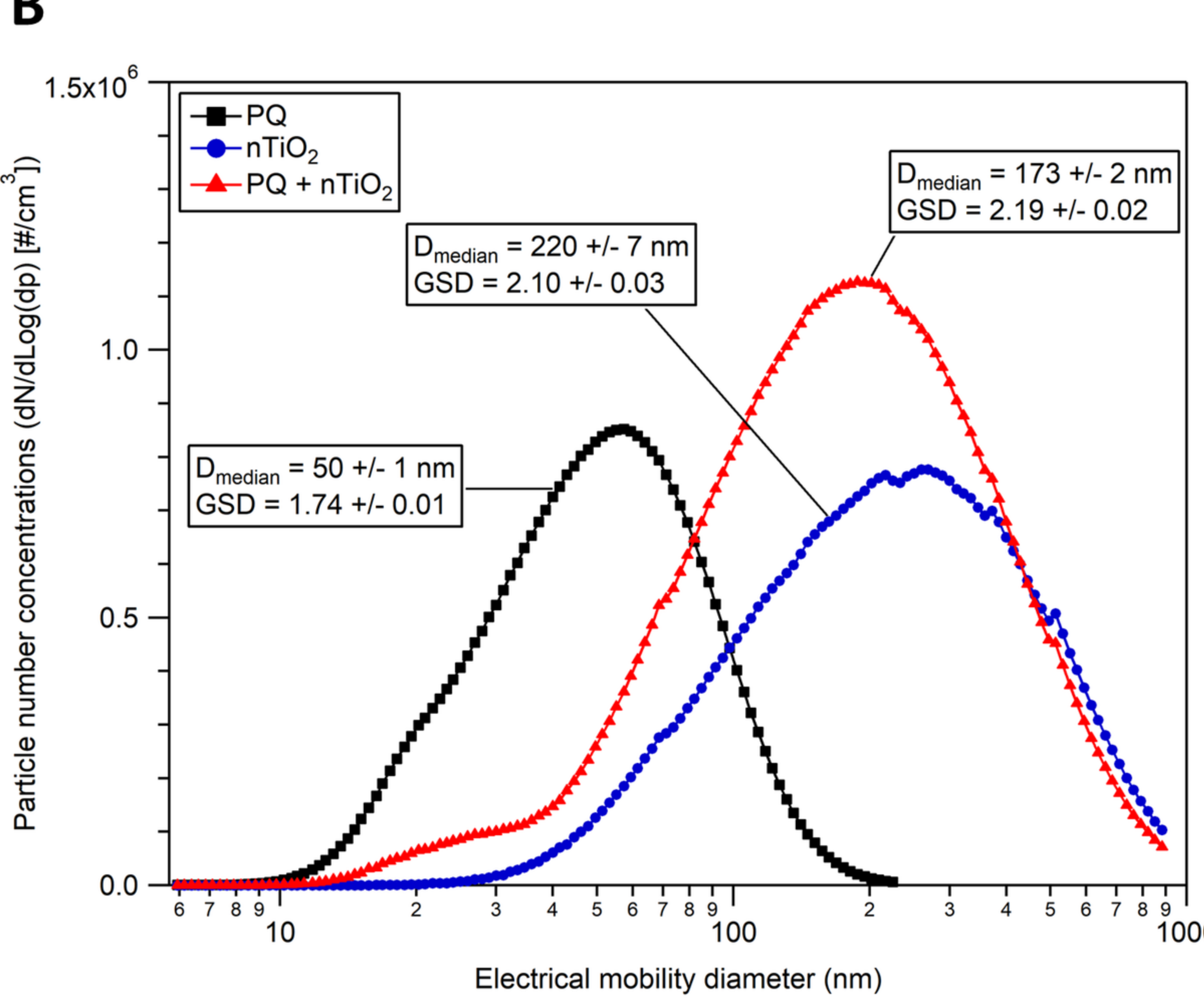
1.5x10^6
1.0
0.5
0.0
PQ
nTiO2
PQ + nTiO2
Dmedian = 50 +/- 1 nm
GSD = 1.74 +/- 0.01
Dmedian = 220 +/- 7 nm
GSD = 2.10 +/- 0.03
Dmedian = 173 +/- 2 nm
GSD = 2.19 +/- 0.02
Particle number concentrations (dN/dLog(dp) [#/cm³])
6 7 8 9
10
2
3
4
5
6
7
8
9
100
2
3
4
5
6
7
8
9
1000
Electrical mobility diameter (nm)

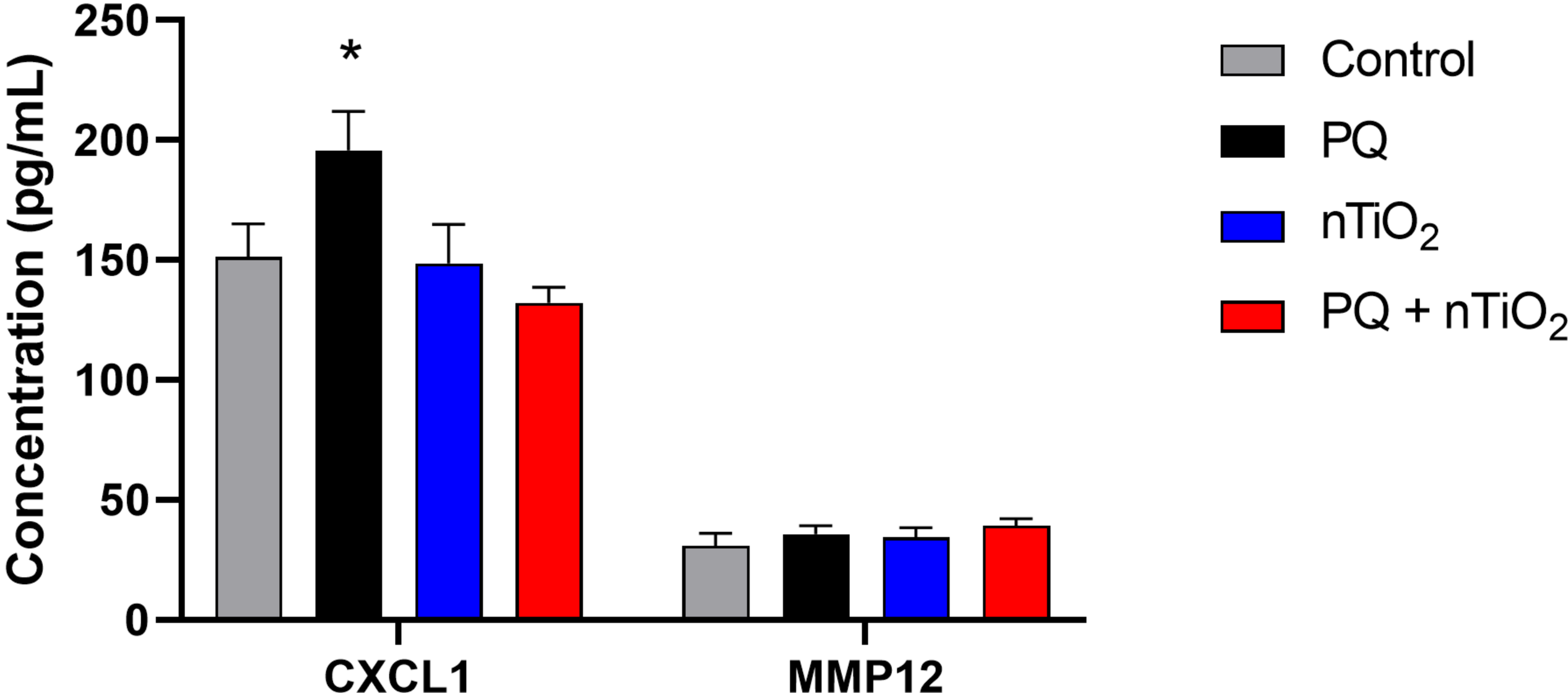
Concentration (pg/mL)
250
200
150
100
50
0
*
CXCL1
MMP12
Control
PQ
nTiO2
PQ + nTiO2

A

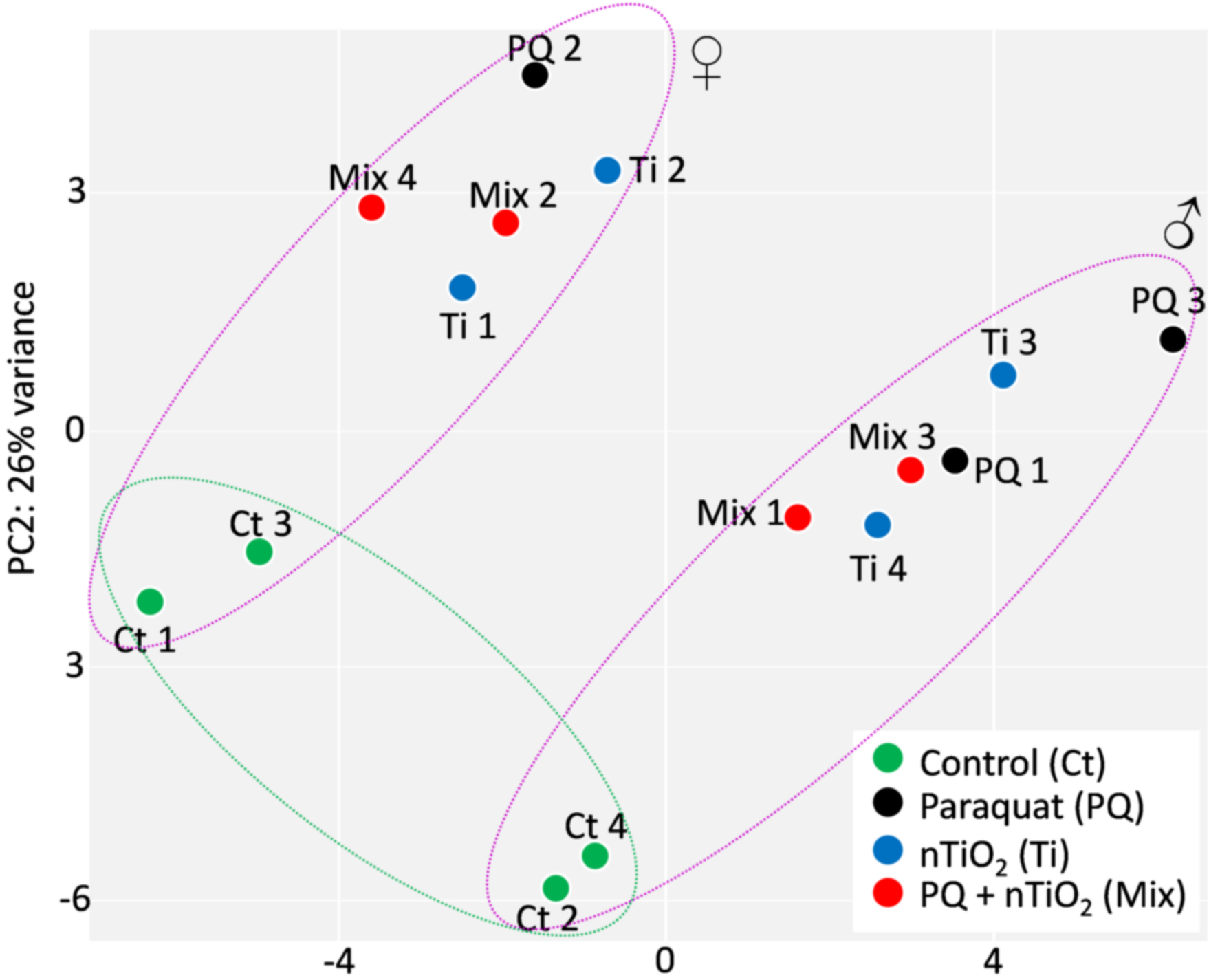

B

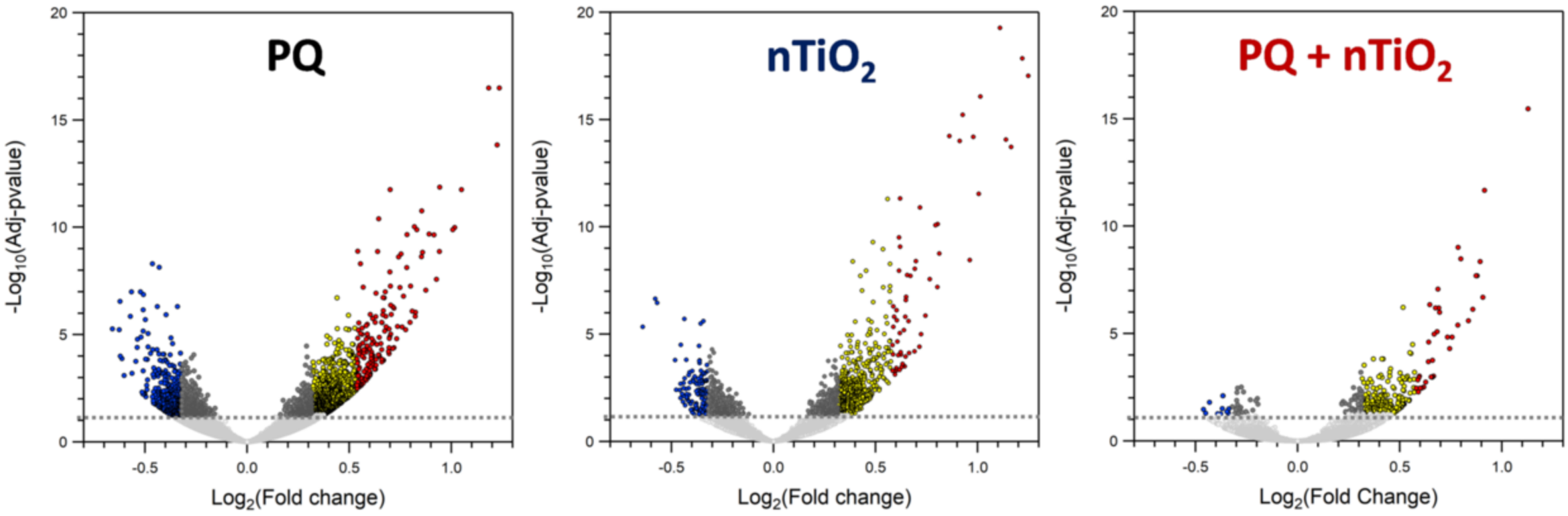

C

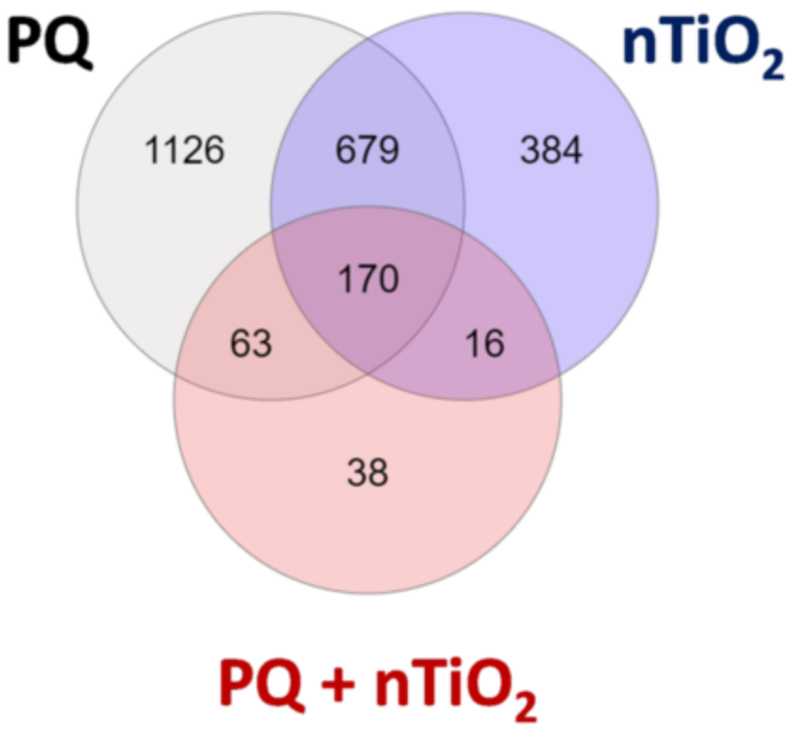

D

Genes	Fold-changes (relative to controls)		
	PQ	$nTiO_2$	PQ + $nTiO_2$
Klhl11	2,35	2,52	1,84
Xkr4	2,27	2,87	2,19
Slc9a7	2,07	2,33	1,83
Nkain3	2,02	2,38	1,69
Lcor	2,01	2,2	1,72
Stxbp5l	1,92	2,16	1,89
Klf12	1,85	1,76	1,59
Chga	1,78	1,88	1,72
Oprm1	1,77	2,24	1,67
Gm38020	1,77	1,95	1,87
Gabrb2	1,76	1,9	1,61
Gm43843	1,72	2,02	1,74
Atn1	1,7	1,51	1,6
Tcp11l1	1,67	1,59	1,57
Gprin3	1,64	1,97	1,62
Chrna4	1,63	1,56	1,56
Camk4	1,58	1,75	1,6
BC005561	1,56	2,01	1,58

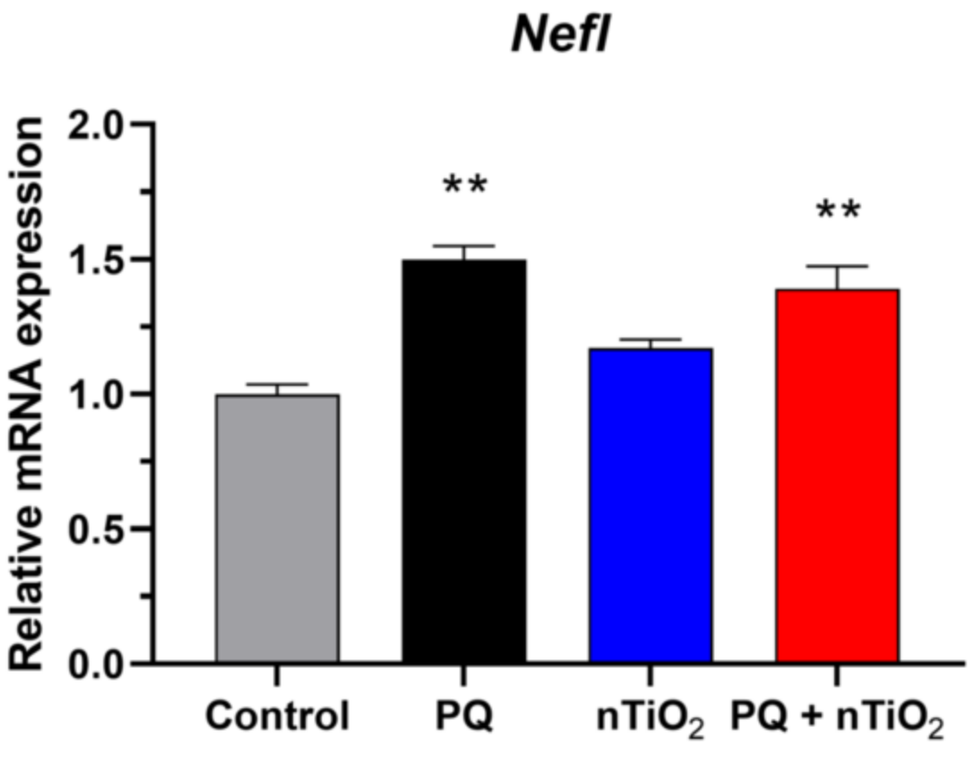
Nefl
Relative mRNA expression
2.0
1.5
1.0
0.5
0.0
**
**
Control
PQ
nTiO2
PQ + nTiO2

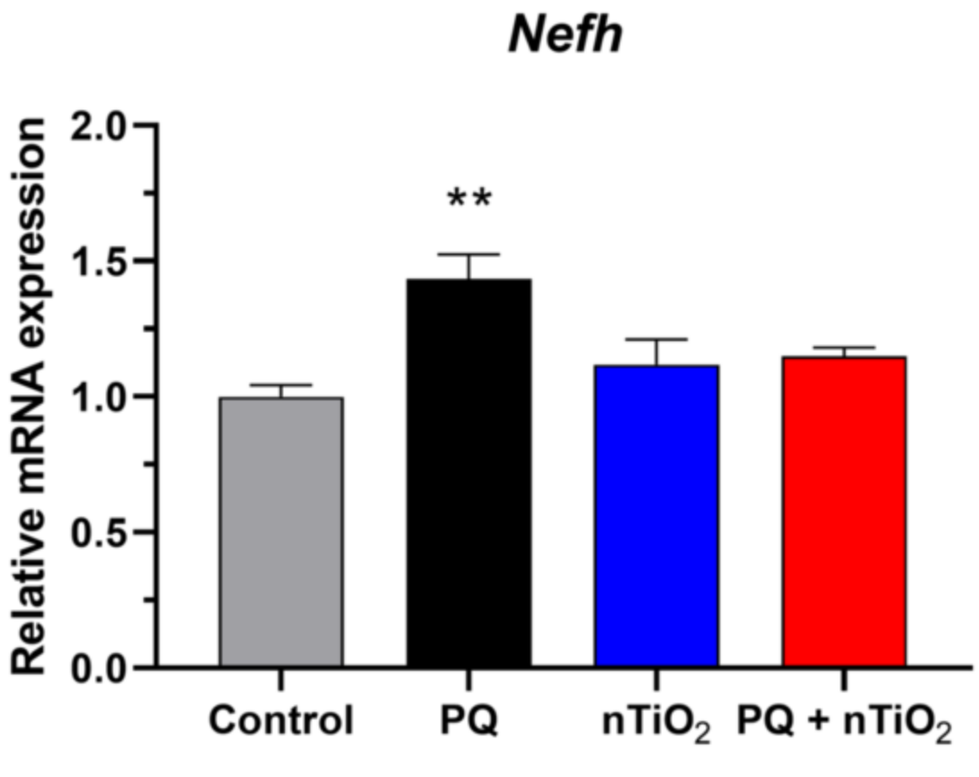
Nefh
Relative mRNA expression
2.0
1.5
1.0
0.5
0.0
**
Control
PQ
nTiO2
PQ + nTiO2

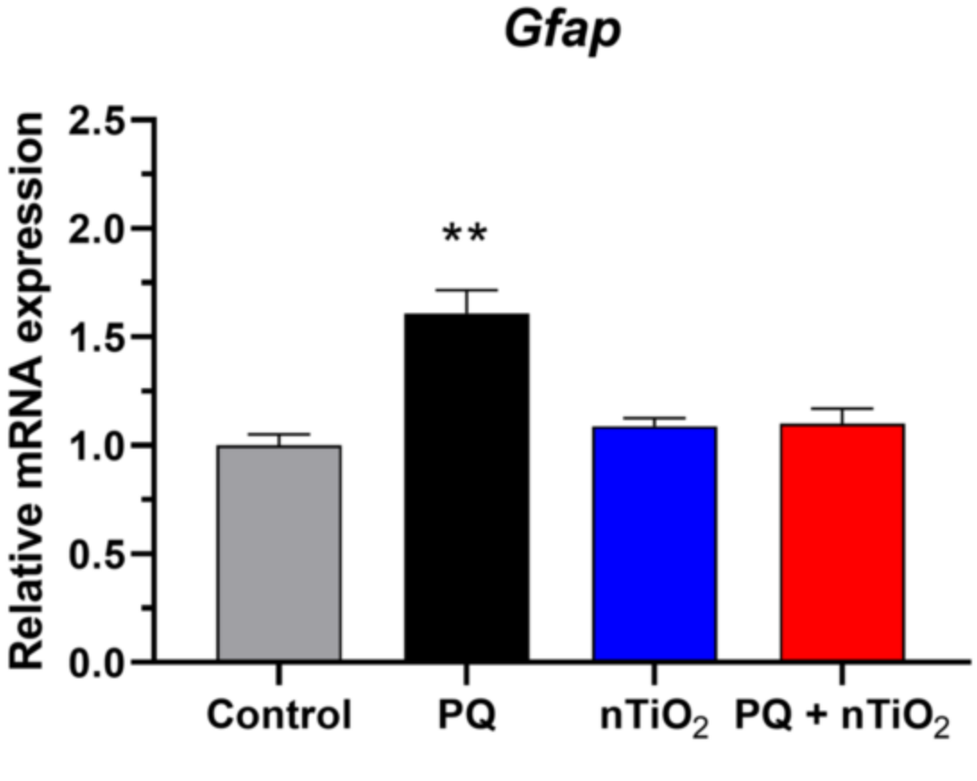
Gfap
Relative mRNA expression
2.5
2.0
1.5
1.0
0.5
0.0
**
Control
PQ
nTiO2
PQ + nTiO2

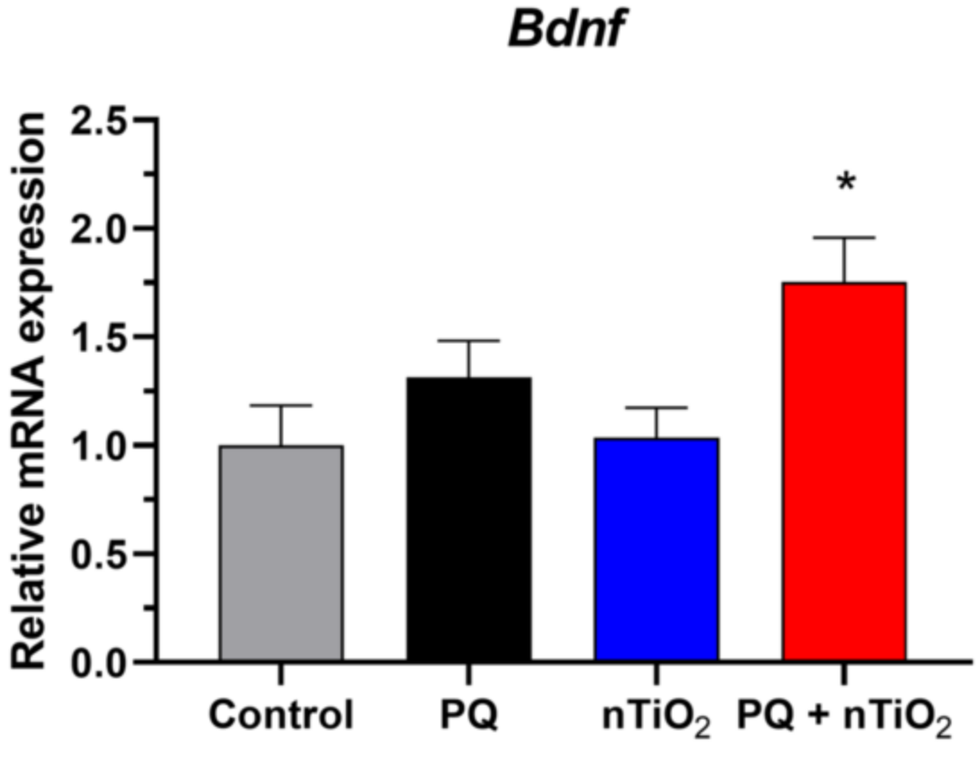
Bdnf
Relative mRNA expression
2.5
2.0
1.5
1.0
0.5
0.0
*
Control
PQ
nTiO2
PQ + nTiO2

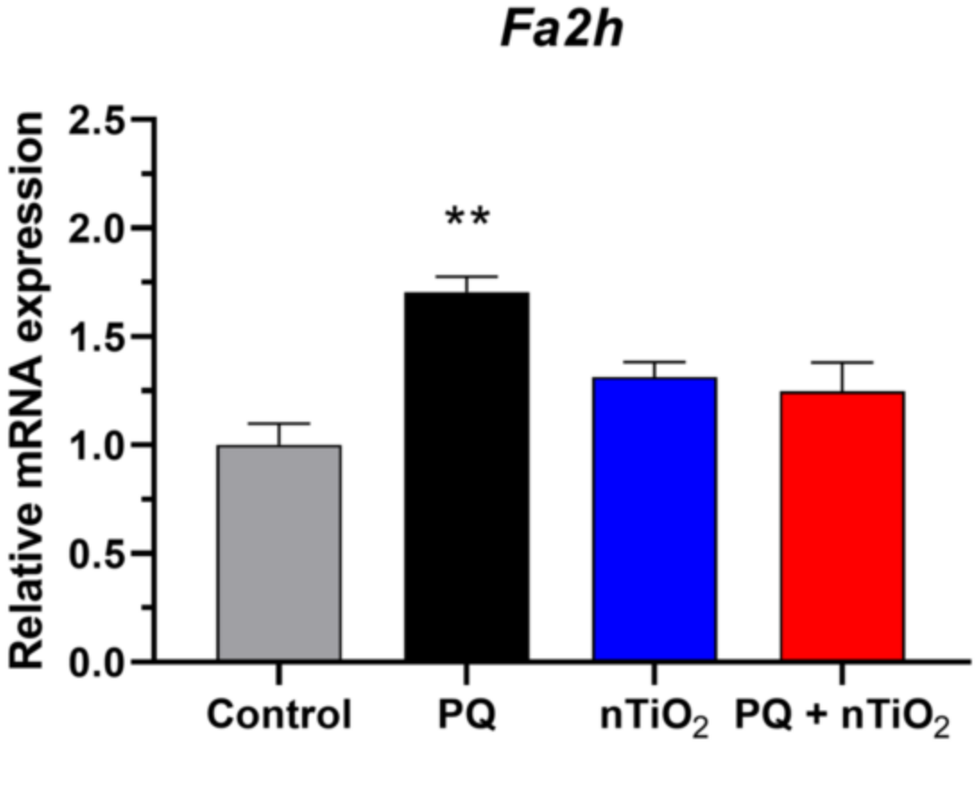
Fa2h
Relative mRNA expression
2.5
2.0
1.5
1.0
0.5
0.0
**
Control
PQ
nTiO2
PQ + nTiO2

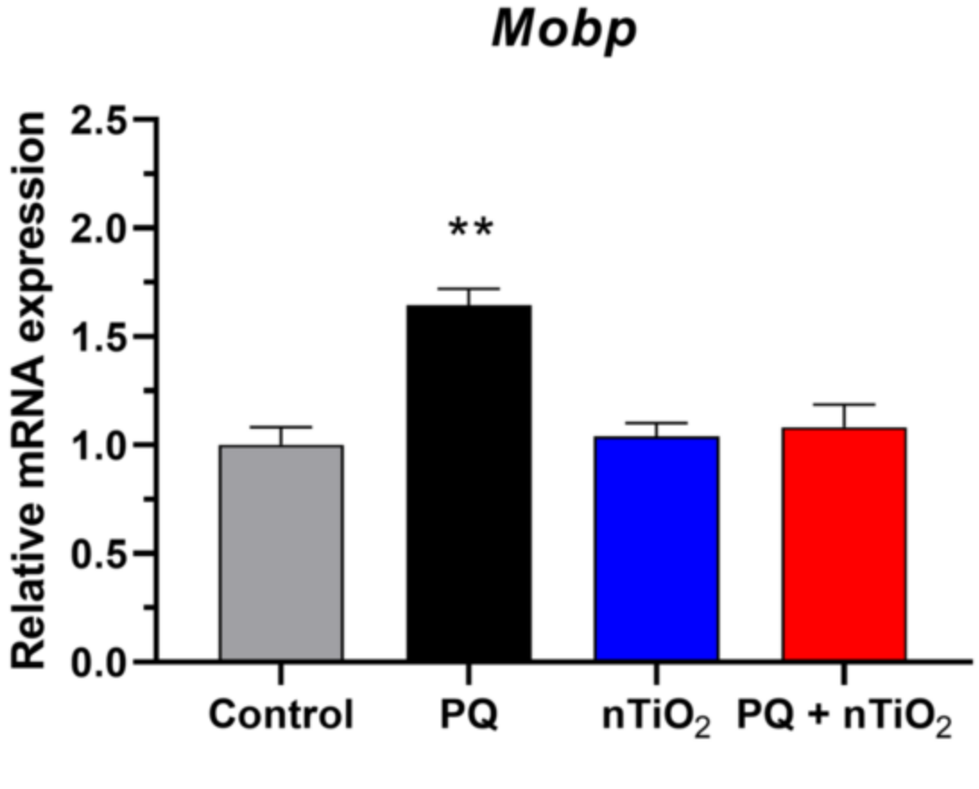
Mobp
Relative mRNA expression
2.5
2.0
1.5
1.0
0.5
0.0
**
Control
PQ
nTiO2
PQ + nTiO2

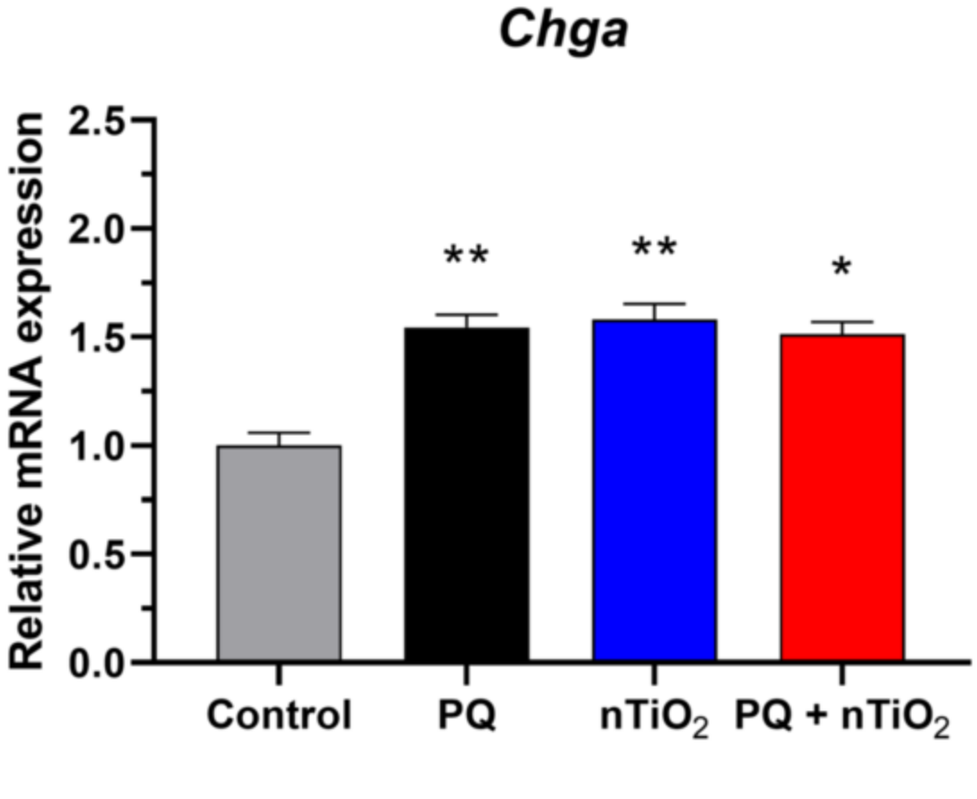
Chga
Relative mRNA expression
2.5
2.0
1.5
1.0
0.5
0.0
**
**
*
Control
PQ
nTiO2
PQ + nTiO2

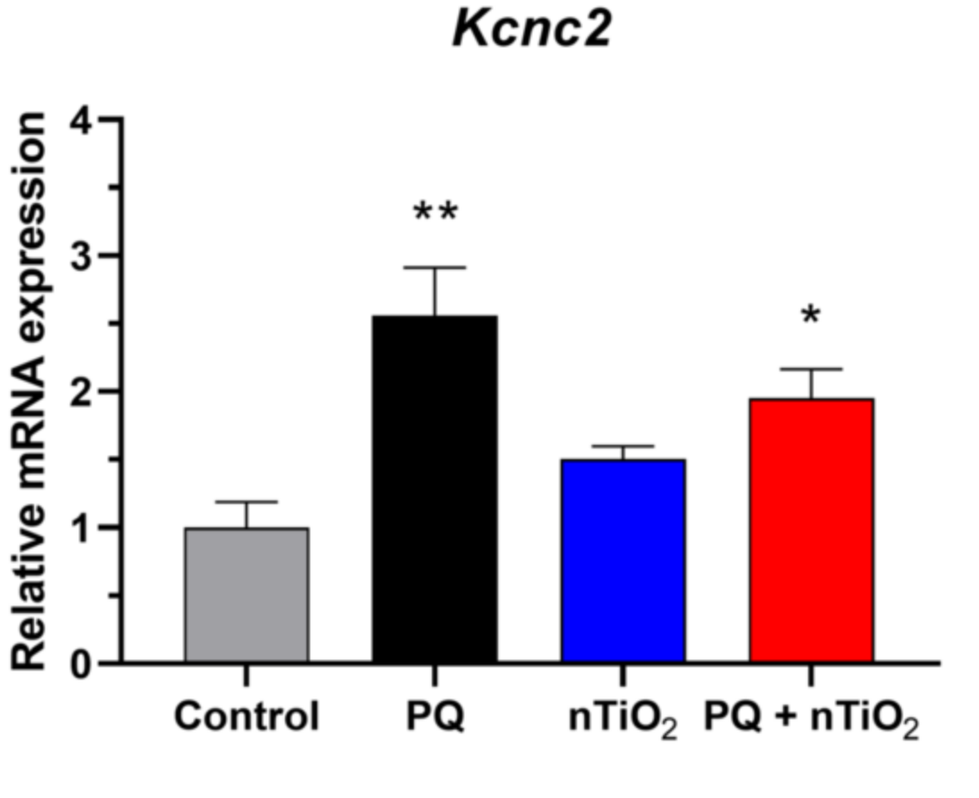
Kcnc2
Relative mRNA expression
4
3
2
1
0
**
*
Control
PQ
nTiO2
PQ + nTiO2

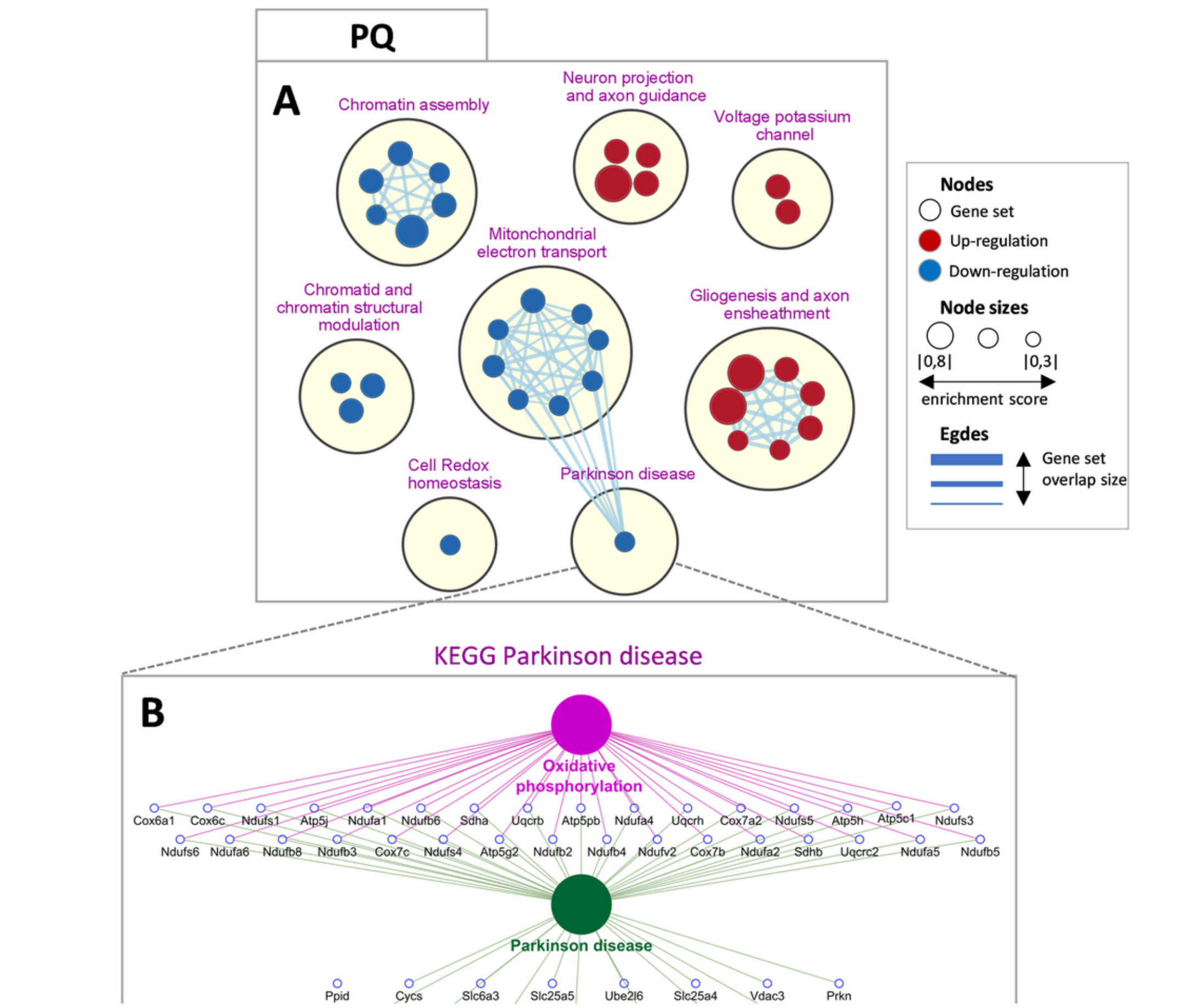
PQ
A
Chromatin assembly
Neuron projection and axon guidance
Voltage potassium channel
Mitonchondrial electron transport
Chromatid and chromatin structural modulation
Gliogenesis and axon ensheathment
Cell Redox homeostasis
Parkinson disease
Nodes
Gene set
Up-regulation
Down-regulation
Node sizes
|0,8|
|0,3|
enrichment score
Egdes
Gene set overlap size
KEGG Parkinson disease
B
Oxidative phosphorylation
Cox6a1 Cox6c Ndufs1 Atp5j Ndufa1 Ndufb6 Sdha Uqcrb Atp5pb Ndufa4 Uqcrh Cox7a2 Ndufs5 Atp5h Atp5c1 Ndufs3
Ndufs6 Ndufa6 Ndufb8 Ndufb3 Cox7c Ndufs4 Atp5g2 Ndufb2 Ndufb4 Ndufv2 Cox7b Ndufa2 Sdhb Uqcrc2 Ndufa5 Ndufb5
Parkinson disease
Ppid Cycs Slc6a3 Slc25a5 Ube2l6 Slc25a4 Vdac3 Prkn

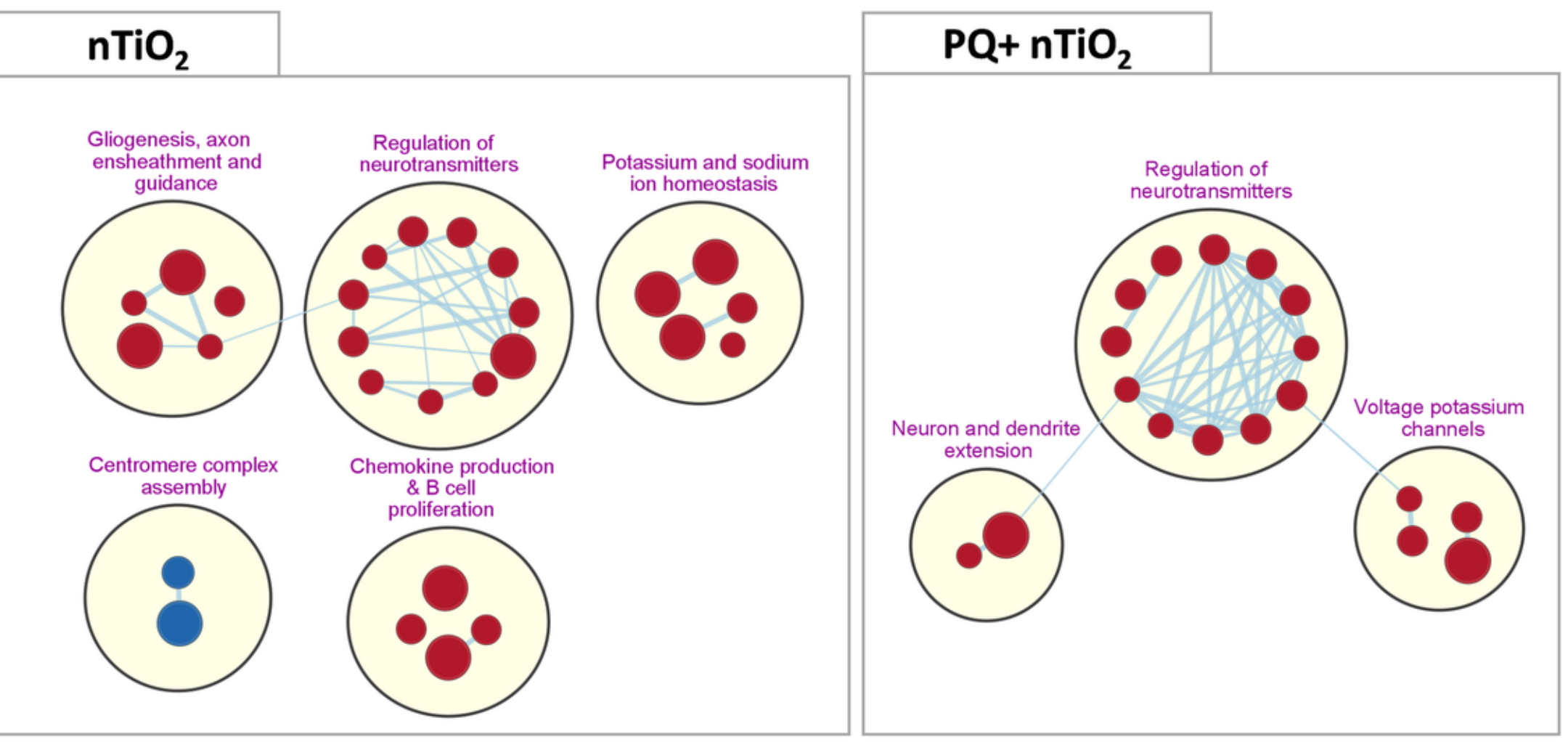
C
nTiO2
Gliogenesis, axon ensheathment and guidance
Regulation of neurotransmitters
Potassium and sodium ion homeostasis
Centromere complex assembly
Chemokine production & B cell proliferation
PQ+ nTiO2
Regulation of neurotransmitters
Neuron and dendrite extension
Voltage potassium channels

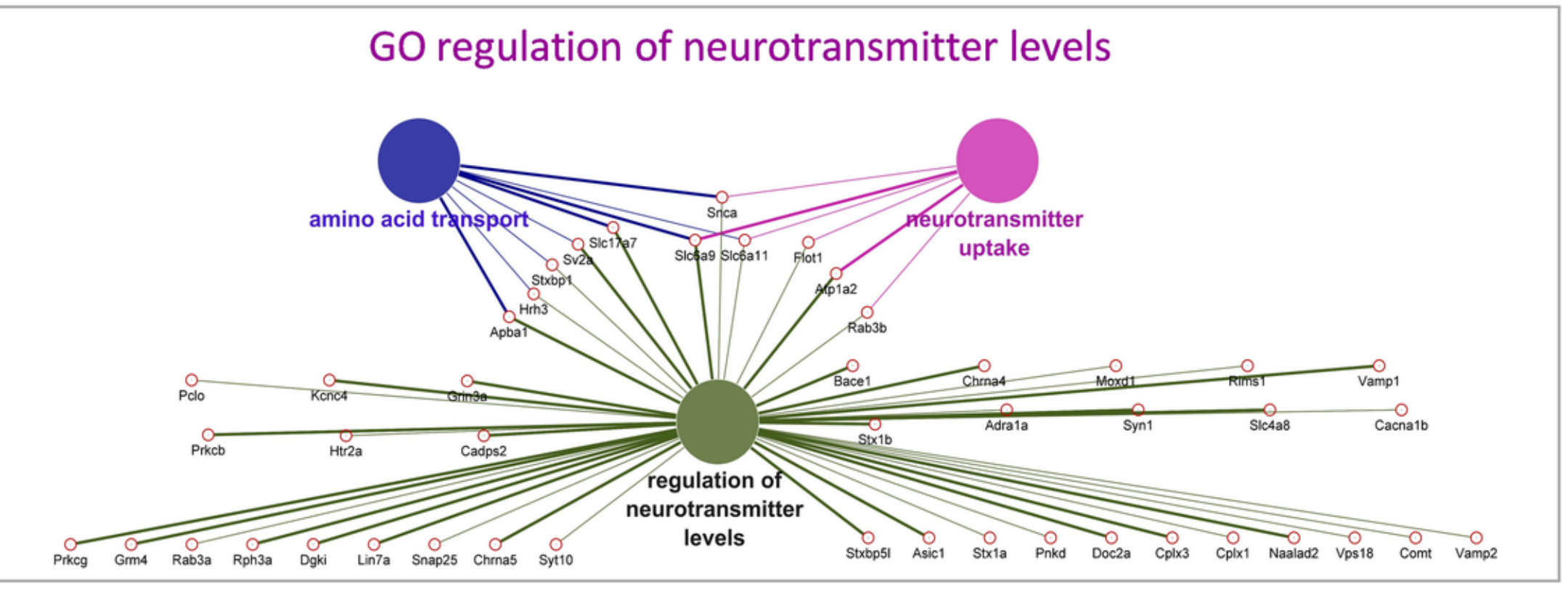
GO regulation of neurotransmitter levels
amino acid transport
neurotransmitter uptake
regulation of neurotransmitter levels
Srica
Slc17a7
Sv2a
Stxbp1
Hrh3
Apba1
Slc6a9
Slc6a11
Flot1
Atp1a2
Rab3b
Pclo
Kcnc4
Grin3a
Prkcb
Htr2a
Cadps2
Bace1
Chrna4
Moxd1
Rims1
Vamp1
Adra1a
Syn1
Slc4a8
Cacna1b
Stx1b
Prkcg
Grm4
Rab3a
Rph3a
Dgki
Lin7a
Snap25
Chrna5
Syt10
Stxbp5l
Asic1
Stx1a
Pnkd
Doc2a
Cplx3
Cplx1
Naalad2
Vps18
Comt
Vamp2

Table 1. Aerosol characteristics

Aerosol	**PQ**	**$nTiO_2$**	**PQ + $nTiO_2$**
Mass concentration (mg/m^3)	*****$[98.7 \pm 3.2] \times 10^{-3}$	10.1 ± 0.6	9.9 ± 0.8
Number concentration [$\times 10^3$ particles/cm^3]	249 ± 17	202 ± 17	308 ± 27
*****Particle median diameter (nm)	50 ± 1	220 ± 7	173 ± 2
*****Geometric standard deviation	1.74 ± 0.01	2.10 ± 0.03	2.29 ± 0.02

Means ± SD are shown. * values which were not were measured during the animal exposure sessions but during the prior metrological characterization of the exposure device.